Inorganic Chemistry

Article

pubs.acs.org/IC

Coordination Polymers Utilizing *N*-Oxide Functionalized Host Ligands

James J. Henkelis,[†] Sarah A. Barnett,[‡] Lindsay P. Harding,[§] and Michaele J. Hardie*,[†]

[†]School of Chemistry, University of Leeds, Woodhouse Lane, Leeds LS2 9JT, U.K.

[‡]Diamond Light Source, Harwell Science and Innovation Campus, Didcot OX11 0DE, U.K.

[§]Department of Chemical and Biological Sciences, University of Huddersfield, Huddersfield HD1 3DH, U.K.

Supporting Information

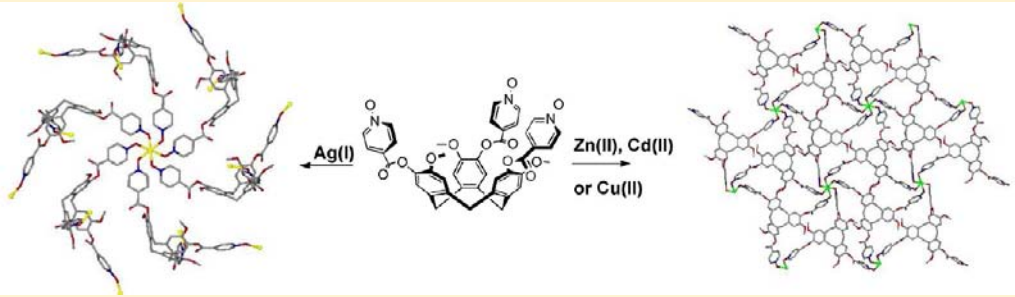

ABSTRACT: Pyridyl functionalized host molecules are oxidized to their *N*-oxide analogues and form a series of coordination polymers and discrete complexes with transition metal cations. Complex $\{[Ag_3(NMP)_6(L1)_2]\cdot 3(ClO_4)\}_\infty$ where L1 = tris(isonicotinoyl-*N*-oxide)cyclotriguaiacylene, NMP = *N*-methylpyrrolidone, is a three-dimensional (3-D) 3,6-connected coordination polymer of pyrite-like (pyr) topology and features ligand unsupported argentophilic interactions, while two-dimensional (2-D) 3,6-connected coordination polymers with the rarely reported kagome dual (kgd) topology are found for $[M(L1)_2]^{2+}$ where M = Zn, Cd, Cu. Ligand L2 = tris(nicotinoyl-*N*-oxide)cyclotriguaiacylene forms a 2-D coordination polymer with 4^4 (sql) grid topology in complexes $\{[M(L2)_2(DMF)_2]\cdot 2ClO_4\cdot 8(DMF)\}_\infty$ M = Cd or Cu, DMF = *N*,*N*′-dimethylformamide, and a double-linked chain structure in $\{[Co(L2)_2(DMF)_2]\cdot 2NO_3\cdot 4(DMF)\cdot H_2O\}_\infty$, and both types of structure feature hand-shake self-inclusion motifs either within or between the polymers. 2-D coordination networks with 6^3 (hcb) topologies are found in complexes $\{[M(L3)(NO_3)_2]\cdot 2(DMF)\}_\infty$ (M = Cd, Zn) and $\{[Cu_5(L3)_2Cl_{10}(NMP)_4]\}_\infty$ where L3 = tris(2-pyridylmethyl)cyclotriguaiacylene, while $[Ag_2(L3)_2(NMP)_4]\cdot 2(BF_4)\cdot 2(NMP)$ has a discrete dimeric structure which again shows hand-shake host–guest interactions supported by π–π stacking.

1. INTRODUCTION

The design and construction of coordination polymers and metal–organic frameworks has rapidly increased in recent years, complexes with regular two-dimensional (2-D) and three-dimensional (3-D) network structures have been assembled through the use of bridging ligand functionality and stereochemical preferences of transition metals as design principles.[1] Potential applications for coordination polymers are far-reaching and have been demonstrated or proposed in the fields of magnetism, nonlinear optics, catalysis, separations and extractions, gas storage, and other zeolitic applications.[1]

Many of the mooted applications of coordination polymers are dependent on their properties as solid state hosts. Their ability to function as hosts is a function of the overall assembly and not the individual molecular or ionic building blocks. Molecular hosts, on the other hand, have an intrinsic ability to bind guest molecules. Cyclic host molecules such as calixarenes or analogues,[2] functionalized cryptophanes,[3] cyclotriveratrylene (CTV),[4] cyclotricatechylene,[5] and a range of tripodal analogues of CTV[6−10] have all been shown to form coordination polymers with embedded molecular recognition sites. Our own work on coordination polymers that incorporate molecular hosts has focused on tripodal CTV-type ligands with monodentate or chelating pyridyl donor groups and a bowl-shaped tribenzo[*a*,*d*,*g*]cyclononatriene core.[7−10] The relative rigidity of the tribenzo[*a*,*d*,*g*]cyclononatriene core means that nominally C_3-symmetric tripodal derivatives are chiral. Despite the ubiquity of carboxylate and other hard-donor ligands in metal–organic framework chemistry,[1] coordination polymers of CTV-type ligands with hard donor atoms are restricted to catecholate ligands[5] and Zheng's recent report of a carboxylic acid functional CTV which forms a nanotube coordination polymer with Cu(II).[6] Other transition metal complexes of carboxylic acid functionalized CTVs have been discrete assemblies.[11]

A simple method of converting soft pyridyl donor ligands to being harder donors is to oxidize them to their *N*-oxide

Received: May 8, 2012
Published: September 27, 2012

   dx.doi.org/10.1021/ic300940k | *Inorg. Chem.* 2012, 51, 10657−10674

analogues. Bridging multifunctional pyridyl-*N*-oxide ligands have been previously reported for coordination polymer synthesis, most particularly with the simple bridging ligand 4,4′-bipyridyl-*N*,*N*′-dioxide.[12] Complicated crystalline assemblies with functionalized calixarenes, bridging pyridyl-*N*-oxides, and transition and lanthanide cations have also been reported.[13] We report herein the conversion of some of our previously reported pyridyl functionalized CTV-types to their *N*-oxide analogues, and their self-assembly with transition metal cations to give coordination polymers and discrete assemblies.

2. RESULTS AND DISCUSSION

2.1. Ligand Synthesis and Their Crystalline Inclusion Chemistry. The *N*-oxide functionalized ligands L1−L4 were

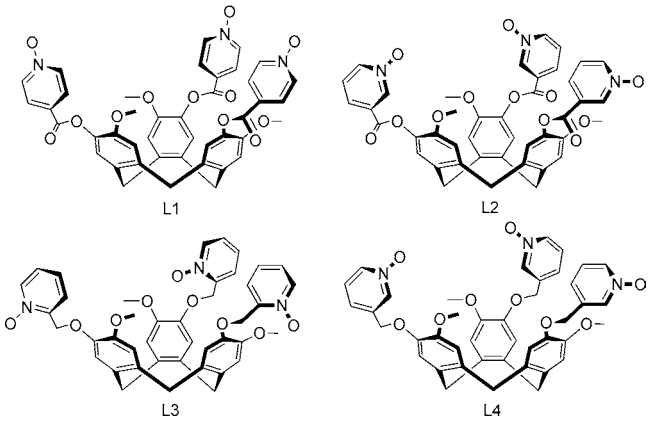

synthesized through oxidation with an excess of *meta*-chloroperoxybenzoic acid (*m*-CPBA) of racemic mixtures of their previously reported pyridyl precursors.[8,14,15] Synthesis of the ester-linked L1 and L2 were performed under an inert atmosphere. Yields were variable, with L2 produced in near quantitative fashion but L4 was only accessible on a small scale and in low 25% yield. Other methods tried included the use of potassium peroxymonosulfate (oxone) and hydrogen peroxide/glacial acetic acid oxidation systems. All ligands showed ^{1}H NMR spectra characteristic of bowl-shaped CTV-type molecules with doublets for both the *endo* and *exo* CH_2 protons of the tribenzo[*a*,*d*,*g*]cyclononatriene core. All ^{1}H and ^{13}C{^{1}H} NMR, mass spectra, IR spectra and elemental analyses were consistent with the proposed structures.

Crystalline clathrate complexes were obtained for L1−L3 from a variety of solvents, and their crystal structures were determined by X-ray diffraction methods, Table 1. Three types of inclusion behavior were observed: clathrate complexes with aligned bowl-in-bowl stacking of the ligand; hand-shake motif self-inclusion; and inclusion of a heteroguest species in the molecular cavity.

Complex L1·DMF, where DMF = *N*,*N*′-dimethylformamide, was obtained from the slow evaporation of a DMF solution of L1. The complex is a clathrate-type inclusion complex where the guest solvent occupies spaces in the crystal lattice formed by packing of the L1 host. The L1 hosts are arranged in perfectly aligned columns, Figure 1a, where the hosts are about 4.7 Å apart which is too long to indicate any $\pi-\pi$ stacking interactions between them. Each column contains only one ligand enantiomer and the orientation of the columns with respect to the L1 bowl, alternates bowl-up, bowl-down. Complex L3·2(H_2O) was obtained from the recrystallization of crude ligand material, using an acetone/diethyl ether mixed solvent system, and also shows perfectly aligned self-stacking of the L3 host molecules and water guests occupying lattice-type

Table 1. Details of Data Collection and Structure Refinements for Clathrate and Inclusion Complexes

	L1·DMF[a]	L2·2NMP	L3·2H_2O	L3·2DMF
formula	$C_{45}H_{40}N_4O_{13}$	$C_{52}H_{51}N_5O_{14}$	$C_{84}H_{86}N_6O_{22}$	$C_{48}H_{53}N_5O_{11}$
Mr	844.81	969.98	1531.59	875.95
crystal color and shape	colorless, plate	colorless, block	colorless, fragment	colorless, needle
crystal size (mm)	0.18 × 0.15 × 0.09	0.20 × 0.12 × 0.12	0.08 × 0.05 × 0.05	0.12 × 0.08 × 0.08
crystal system	monoclinic	triclinic	triclinic	triclinic
space group	$P2_1/n$	$P\bar{1}$	$P1$	$P\bar{1}$
a (Å)	4.6996(16)	13.1282(13)	4.5584(6)	9.2161(5)
b (Å)	21.173(7)	14.0590(15)	16.3294(18)	11.1018(7)
c (Å)	39.052(14)	15.0060(13)	24.986(3)	22.8800(15)
α (deg)	90	92.776(6)	99.660(4)	85.589(4)
β (deg)	91.286(4)	95.507(7)	92.270(4)	81.494(3)
γ (deg)	90	95.507(7)	92.770(4)	75.676(3)
V (Å^3)	3885(2)	2447.2 (4)	1829.2(4)	2241.3(2)
Z	4	2	1	2
ρ_{calc} (g.cm^{-3})	1.444	1.316	1.390	1.298
θ range (deg)	1.78−31.70	1.6−25.00	2.25−24.98	1.80−30.10
no. data collected	36804	20244	22009	44701
no. unique data	12838	8581	11097	12918
R_{int}	0.0510	0.0586	0.0813	0.0564
no. obs. data ($I > 2\sigma(I)$)	8287	4367	6454	6881
no. parameters	564	567	1016	584
no. restraints	0	1	3	0
R_1 (obs data)	0.0652	0.1075	0.0876	0.0554
wR_2 (all data)	0.1653	0.3754	0.2440	0.1312
S	1.083	1.192	0.988	0.995

[a]Data collected using synchrotron radiation.

dx.doi.org/10.1021/ic300940k | *Inorg. Chem.* 2012, 51, 10657−10674

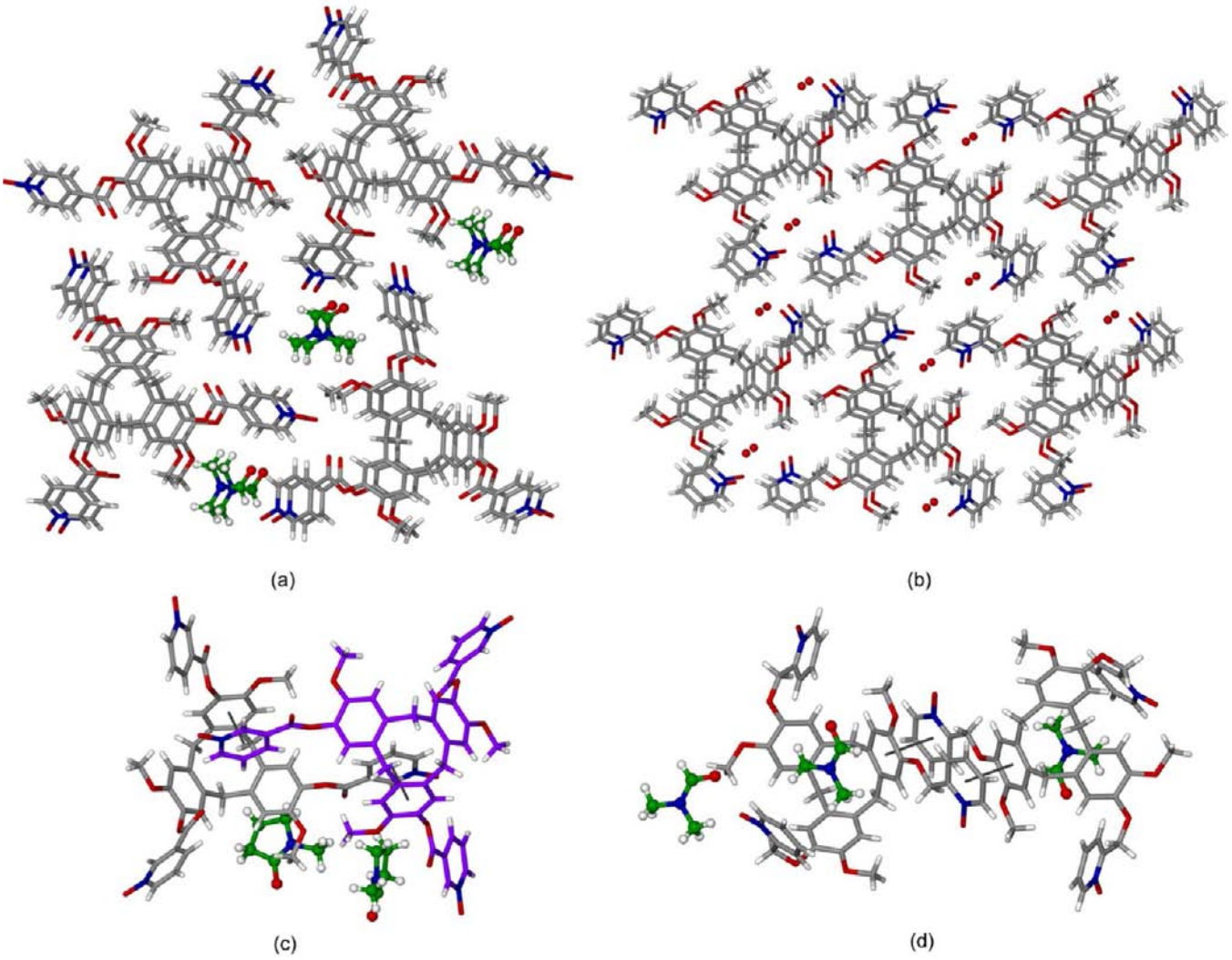

Figure 1. Crystal structures of crystalline clathrate and inclusion compounds. (a) L1·DMF clathrate exhibiting bowl-in-bowl stacking; (b) the polar L3·2(H_2O) clathrate where all stacks of ligand are in the same orientation; (c) L2·2NMP clathrate showing hand-shake motif, only one position of a disorder of one side arm is shown; (d) L3·2(DMF) inclusion complex. Face-to-face $\pi-\pi$ stacking interactions are indicated by thin lines.

guest positions, Figure 1b. Both L3 enantiomers are present in the structure and each column is homochiral. Unlike for L1·DMF however, the structure of L3·2(H_2O) is polar, with all columns of L3 having the same orientation with respect to molecular bowl. Aligned self-stacking of CTV-type molecules has been previously observed in crystal structures, and is indicated by a short unit cell length equivalent to the stacking distance of about 4.5−4.7 Å.[14,16]

The complex L2·2(NMP) where NMP = *N*-methylpyrrolidone was obtained from diffusion of diethyl ether vapors into a NMP solution of L2. This also a clathrate type inclusion complex with the NMP guests occupying positions in the crystal lattice created by packing of the host L2. L2 molecules form a different type of self-complementary interaction where one 3-pyridyl-*N*-oxide group of a L2 host is directed into the molecular cavity of another L2 ligand though with its polar *N*-oxide group pointing outward, and vice versa, Figure 1c. This type of pairwise association is known as the hand-shake motif, and is a relatively common motif in crystalline structures of CTV-type hosts, both in clathrate complexes,[9,10,17] within discrete assemblies and one-dimensional (1-D) coordination chains,[9] and between 2-D networks.[10] It has also been reported for crystalline clathrate complexes of other types of host molecule.[18] In this example, there are both face-to-face $\pi-\pi$ stacking interactions between the 3-pyridyl-*N*-oxide and a phenyl group of the tribenzo[*a*,*d*,*g*]cyclononatriene host core at ring centroid separations 3.79 Å, along with C−H···π interactions to the other host phenyl rings. An isomorphic clathrate complex can be obtained with DMF (unit cell, triclinic, $P\bar{1}$, a = 12.796(5), b = 13.8428(6), c = 15.1063(6) Å, α = 116.953(2), β = 91.260(2), γ = 96.118(2)°).

The inclusion complex L3·2(DMF) was obtained by diffusion of diethyl ether vapors into a DMF solution of L3. In this complex, one DMF molecule occupies a lattice-type guest position while the other is the intracavity guest for the L3 host, Figure 1d. The L3 ligand does not have approximate C_3 symmetry with one extended arm oriented in toward the guest DMF. Intracavity guest binding of small organic guest molecules has also been reported with other CTV-type hosts.[19] The {L3∩DMF} complexes form pairwise back-to-back $\pi-\pi$ stacking interactions with a ring centroid separation of 3.57 Å, Figure 1d.

2.2. Transition Metal Complexes. The ligands L1-L4 were reacted with a variety of transition metal salts, including

dx.doi.org/10.1021/ic300940k | *Inorg. Chem.* 2012, 51, 10657−10674

both hard and soft metal ions and counter-anions ranging from strongly to weakly coordinating. Single crystals were grown by diffusion of diethyl ether vapors into NMP or DMF solutions of metal salts and ligand mixtures, and their structures determined by X-ray techniques, Table 2. Single crystals were only isolated with ligands L1-L3 but not with L4. The majority of the isolated complexes were coordination polymers with 2-D polymers predominating.

The complexes obtained show a number of different motifs. The highest anticipated network connectivity is 3,6-connected with the ligand as the 3-connecting node and metal ion the 6-connecting node. This is found for a series of complexes with L1 in both 3-D and 2-D frameworks. In complexes of L2 and L3 lower connectivity is observed for the metal ion, the ligand or both. When the ligand shows lower than anticipated 3-connectivity then the polymeric or discrete complexes formed display self-complementary inclusion motifs involving the cavitand ligand.

2.2.1. Coordination Polymers of 3,6-Connectivity. Coordination polymers with the anticipated 3,6-connectivity were formed with ligand L1 in the complexes $\{[Ag_3(NMP)_6(L1)_2]\cdot 3(ClO_4)\cdot n(NMP)\}_\infty$ **1**, $\{[Zn(L1)_2]\cdot 2(BF_4)\cdot n(NMP)\}_\infty$ **2**, $\{[Co(L1)_2]\cdot 2(BF_4)\cdot n(DMF)\}_\infty$ **3**, and $\{[Cu(L1)_2]\cdot[Cu(H_2O)(NMP)_4]\cdot 4(BF_4)\cdot 8(NMP)\cdot 2(H_2O)\}_\infty$ **4**. Of these, complex **1** has a 3-D coordination polymer structure while **2**−**4** are 2-D.

The structure of $\{[Ag_3(NMP)_6(L1)_2]\cdot 3(ClO_4)\cdot n(NMP)\}_\infty$ **1** was solved in the cubic space group $Pa\bar{3}$. There are two crystallographically distinct Ag ions, one located on a 3-fold inversion axis (Ag1) and the other on a 3-fold rotation axis (Ag2). The remainder of the asymmetric unit consists of one-third of a L1 ligand, an NMP ligand, and half a disordered perchlorate counteranion. Selected bond lengths and angles are given in Table 3. Ag1 is coordinated by one pyridyl-*N*-oxide group of six symmetry equivalent L1 ligands in a distorted octahedral fashion, Figure 2a. There is further interaction to two Ag2 ions through ligand-unsupported argentophilic interactions with Ag···Ag separation 3.2753(9) Å. This is consistent with previous reports of unsupported argentophilic interactions where Ag···Ag distances are typically in the range 2.9 to 3.3 Å.[20−22] The Ag_3 argentophilic trimer in complex **1** is centrosymmetric and exactly linear. Examples of complexes with linear trimers of Ag(I) are relatively rare and most reported crystal structures of such complexes involve ligand-supported argentophilic interactions.[23] To the best of our knowledge, there have only been two other examples of unsupported argentophilic linear trimers, in the cationic complexes $[\{Ag(1,10\text{-phenanthroline})_2\}_3]^{3+}$[21] and $[Cd(imidazolyl)_5\text{-}\mu\text{-}(CN)\text{-}Ag(CN)\text{-}Ag(CN)_2\text{-}Ag(CN)\text{-}\mu\text{-}(CN)\text{-}Cd(imidazolyl)_5]^+$.[22] Each Ag2 ion in complex **1** is further coordinated by three symmetry-equivalent *N*-methylpyrrolidone ligands at Ag−O distance 2.414(6) Å and has an approximately tetrahedral coordination environment, Figure 2a.

Each L1 ligand within **1** is centered around a crystallographic 3-fold axis and bridges between three Ag1 ions, Figure 3b. The Ag2 ions are not involved in any ligand bridging interactions and do not play a role in the network topology. They are located on the same 3-fold axes as the L1 ligands, and the $\{(Ag2)(NMP)_3\}$ moieties are found to the outside of the host cavity, Figure 2c. The 3-D coordination polymer formed between Ag1 ions and L1 has 3,6-connectivity with a pyrite-like (**pyr**) network, Figure 2.[24] The **pyr** net has Schläfli symbol $(6^3)_2(6^{12}.8^3)$ and features 6-gons and 8-gons within the net.[25]

In the overall crystal lattice there are no significant channels within the structure of **1**. There are, however, large oval-shaped cavities which are bound along their long axis by two L1 ligands facing each other in a head-to-head fashion, as shown in Figure 2a. The distance between these two L1 ligands is about 30 Å, as measured between the centers of the three methylene carbon atoms for each ligand. This cavity contains disordered perchlorate anions and disordered NMP solvent, with the latter not located crystallographically. Thermal gravimetric analysis (TGA) of complex **1** shows a loss of 40% weight up to about 210 °C. This is consistent with the loss of all NMP ligands, along with a further eight NMP solvent molecules per formula unit. Voids within the crystal lattice are consistent with this level of solvation.

The complexes $\{[Zn(L1)_2]\cdot 2(BF_4)\cdot n(NMP)\}_\infty$ **2**, $\{[Co(L1)_2]\cdot 2(BF_4)\cdot n(DMF)\}_\infty$ **3**, and $\{[Cu(L1)_2]\cdot[Cu(H_2O)(NMP)_4]\cdot 4(BF_4)\cdot 8(NMP)\cdot 2(H_2O)\}_\infty$ **4** all feature $[M(L1)_2]^{2+}$ coordination polymers which, unlike the pyrite-related 3,6-connected network of $[Ag_3(NMP)_6(L1)_2]^{3+}$, have a 2-D kagome dual topology. These complexes were highly solvated, with complexes **2** and **3** being very weakly diffracting and synchrotron radiation necessary to collect suitable X-ray data for **2**. For both **2** and **3** only the positions of the $[M(L1)_2]^{2+}$ units could be established within their unit cells. While complexes **2**−**4** show essentially the same coordination polymer structure, they are not structurally isomorphic.

$\{[Zn(L1)_2]\cdot 2(BF_4)\cdot n(NMP)\}_\infty$ **2** crystallizes in a triclinic cell and the Zn center is found on an inversion center. It has octahedral coordination, being coordinated by six symmetry-equivalent L1 ligands. Each L1 ligand coordinates to three symmetry-equivalent Zn ions thus forming a 3,6-connected network, Figure 4. The kagome dual structure or **kgd** topology[24] resembles a star-shaped tessellation of diamonds and has the Schlafli symbol $(4^3)_2.(4^6.6^6.8^3)$.[25] The network is not flat but has two tiers of L1 ligands inverted with respect to one another and with their molecular cavities oriented inward to give a concave-convex aspect to the net.

Complex $\{[Co(L1)_2]\cdot 2(BF_4)\cdot n(DMF)\}_\infty$ **3** has higher symmetry than **2**, crystallizing in a monoclinic unit cell with the Co(II) ion situated on an inversion center. It likewise forms a $[Co(L1)_2]^{2+}$ 3,6-connected coordination polymer of **kgd** topology. The main difference between the two networks is that, while in **2** the L1 ligand had approximate and noncrystallographic C_3 symmetry with all of the ligand arms in roughly the same orientation, the same is not the case in **3** as one pyridylmethyloxy moiety is disordered across two positions (see Supporting Information). The coordination geometry about the metal is closer to true octahedral than in **2**, Table 3.

There are large tube-like channels apparent within the networks running down the *a* and *b* unit cell axes for both **2** and **3** alike. Further channels are created through the packing of the networks in the 3-D lattice. In complex **2** the 2-D networks are related by translations, while in **3** they are related by a screw axis; however, both exhibit interlayer channels of similar size and shape, Figure 5. The overall solvent accessible space within the structure accounts for about 2/3 of the unit cell volume for each complex. The location of solvent molecules and counter-anions could not be established with the single crystal X-ray data. Powder XRD studies indicated that, in both cases, the structure collapses on evacuation of solvent with the material losing crystallinity. TGA of **2** shows a stepwise mass loss of 35% to about 215 °C (see Supporting Information). This is in agreement with the loss of about 10 molecules of solvent *N*-

Table 2. Details of Data Collection and Structure Refinements for Coordination Complexes

	1	2[a]	3	4	5	7	8
formula	$C_{114}H_{120}Ag_3Cl_3N_{12}O_{42}$	$C_{84}H_{66}BF_4N_6O_{24}Zn$	$C_{84}H_{66}BCoF_4N_6O_{24}$	$C_{144}H_{180}B_4Cu_2F_{16}N_{18}O_{39}$	$C_{48}H_{53}CdN_7O_{17}$	$C_{124}H_{150}Cl_{10}Cu_5N_{14}O_{26}$	$C_{48}H_{51}Cl_2CuN_5O_{16}$
Mr	2760.18	1695.61	1689.17	3261.38	1112.37	2924.78	1088.38
crystal color and shape	colorless, needle	colorless, plate	orange, plate	green, plate	colorless, needle	green, needle	green, block
crystal size (mm)	0.12 × 0.06 × 0.04	0.20 × 0.12 × 0.12	0.18 × 0.08 × 0.08	0.16 × 0.08 × 0.08	0.18 × 0.13 × 0.13	0.15 × 0.12 0.04	0.18 × 0.16 × 0.16
crystal system	cubic	triclinic	monoclinic	triclinic	monoclinic	triclinic	triclinic
space group	$Pa\bar{3}$	$P\bar{1}$	$C2/c$	$P\bar{1}$	$P2_1$	$P\bar{1}$	$P\bar{1}$
a (Å)	25.9744(8)	17.44(3)	17.5839(18)	18.1713(19)	8.0052(7)	11.7843(8)	12.5748(18)
b (Å)	25.9744(8)	17.54(4)	29.7518(18)	21.487(2)	24.325(2)	18.9058(12)	14.424(2)
c (Å)	25.9744(8)	18.13(3)	34.404(3)	24.177(2)	14.2675(12)	24.2187(16)	18.045(3)
α (deg)	90	100.28(8)	90	84.788(4)	90.00	100.396(3)	72.077(7)
β (deg)	90	101.91(6)	99.609(3)	80.734(4)	100.117(3)	101.476(3)	71.966(6)
γ (deg)	90	118.80(6)	90	80.361(4)	90.00	97.089(3)	88.086(7)
V (Å^3)	17524.1(9)	4499(15)	17746(3)	9165.1(16)	2735.0(4)	5129.5(6)	2954.3(8)
Z	4	1	4	2	2	1	2
ρ_{calc} (g.cm^{-3})	1.046	0.626	0.632	1.182	1.351	0.947	1.224
θ range (deg)	1.36−25.00	1.31− 22.69	1.36−20.00	1.33−25.00	1.67−29.36	4.08−24.93	1.62−26.37
no. data collected	70296	30886	43822	104252	20183	61475	12957
no. unique data	5148	12825	8276	32232	12571	17543	5791
R_{int}	0.0603	0.0728	0.0976	0.0536	0.0279	0.0377	0.0433
no. obs. Data ($I > 2\sigma(I)$)	3178	4800	3347	18025	10482	11995	3678
no. parameters	275	523	384	1768	654	815	646
no. restraints	1	0	3	23	1	0	0
R_1 (obs data)	0.0958	0.0729	0.0909	0.1643	0.0583	0.0614	0.1202
wR_2 (all data)	0.2982	0.1992	0.2605	0.4894	0.1705	0.1991	0.3810
S	1.074	0.805	0.881	1.751	1.036	1.032	1.445

	9	10	11	12[a]
formula	$C_{114}H_{132}Ag_2B_2F_8N_{12}O_{24}$	$C_{114}H_{136}CdCl_2N_{16}O_{42}$	$C_{114}H_{136}Cl_2CuN_{16}O_{42}$	$C_{102}H_{110}CoN_{14}O_{36}$
Mr	2443.68	2585.69	2536.83	2166.97
crystal color and shape	colorless, block	colorless, block	green, block	orange, needle
crystal size (mm)	0.18 × 0.14 × 0.12	0.20 × 0.12 × 0.12	0.22 × 0.10 × 0.10	0.10 × 0.05 × 0.05
crystal system	monoclinic	monoclinic	monoclinic	triclinic
space group	$P2_1/c$	$P2_1/n$	$P2_1/n$	$P\bar{1}$
a (Å)	22.0843(11)	16.2283(13)	16.2126(14)	12.047(5)
b (Å)	12.7697(7)	19.5779(17)	19.3231(17)	14.724(6)
c (Å)	21.5212(11)	20.2184(15)	19.8240(17)	18.024(7)
α (deg)	90.00	90.00	90	97.0790(10)
β (deg)	111.184(2)	99.773(4)	100.091(2)	107.478(5)
γ (deg)	90.00	90.00	90	102.281(7)
V (Å^3)	5659.1(5)	6330.5(9)	6114.3(9)	2919(2)
Z	2	2	2	1
ρ_{calc} (g.cm^{-3})	1.434	1.356	1.378	1.233
θ range (deg)	1.91−23.60	1.82−31.21	1.48−29.51	1.17−22.50
no. data collected	19444	72930	58430	33933

dx.doi.org/10.1021/ic300940k | *Inorg. Chem.* 2012, 51, 10657−10674

Table 2. continued

	9	10	11	12[a]
no. unique data	8388	20393	16595	8349
R_{int}	0.0385	0.0426	0.0549	0.0241
no. obs. data ($I > 2\sigma(I)$)	5794	14902	11350	7859
no. parameters	641	803	803	649
no. restraints	12	0	0	0
R_1 (obs data)	0.0941	0.0425	0.0470	0.1207
wR_2 (all data)	0.3055	0.1227	0.1258	0.4064
S	1.043	1.020	1.017	1.995

[a]Data collected using synchrotron radiation.

methylpyrrolidone per formula unit, and the channel size is consistent with high levels of solvation.

Complex $\{[Cu(L1)_2]\cdot[Cu(H_2O)(NMP)_4]\cdot 4(BF_4)\cdot 8(NMP)\cdot 2(H_2O)\}_\infty$ **4** features both a kagome dual $[M(L1)_2]^{2+}$ coordination polymer, and a mononuclear $[Cu(H_2O)(NMP)_4]^{2+}$ complex. Complex **4** crystallizes with a triclinic unit cell and, unlike in complexes **2** and **3**, good quality X-ray data could be obtained which allowed for the location and refinement of several solvent molecules and three of the four counter-anions. There are two crystallographically independent Cu ions in the $[Cu(L1)_2]^{2+}$ network both of which are placed on an inversion center, and have distorted octahedral geometry typical of Jahn−Teller elongations, Table 3. The two crystallographically independent L1 ligands within the network are differentiated by one ligand having one ester group rotated 180° with respect to the others so that the carbonyl is pointed into the molecular cavity of the ligand. They also each show different host−guest motifs: one L1 has a solvent NMP in the intracavity position; while the other has a complexed NMP from the discrete $[Cu(H_2O)(NMP)_4]^{2+}$ complex taking up the guest position, Figure 6. In both cases the hydrophobic $-CH_2-$ groups of the NMP are directed into the cavity. The $[Cu(H_2O)(NMP)_4]^{2+}$ complex has a distorted square pyramidal structure with the longest Cu3−O distance at the apical position, Table 3. The largest O−Cu−O angles are 169.2(3) and 157.3(3)°, giving a τ of about 0.2, indicative of square pyramidal geometry.[26] Packing of the networks in the 3-D lattice is similar to that seen for complex **2** and the apparent channels are occupied by additional NMP and counter-anions (see Supporting Information).

A notable feature of these structures is the relative rarity of known examples of coordination polymers with these topologies. Most reported examples of 3-D 3,6-connected networks are related to rutile (**rt1**),[27] and the pyrite structure is much rarer.[28] Prior examples of the kagome dual structure within coordination polymers are also restricted,[29−33] although the topology is found in the structure of CdI_2 and other inorganic salts. The closest examples of kagome dual structures to those reported here are the networks of $[Cd(2,4,6\text{-tris}[4\text{-}(1H\text{-imidazole-1-yl})phenyl]\text{-}1,3,5\text{-triazine})_2]^{2+}$ reported by Su and co-workers,[29] and an example reported by Gao and co-workers where the network included trinuclear $[Mn_3(\mu_3\text{-}F)]$ clusters and mononuclear octahedral Mn(II).[30] In both of these examples a similar concave-convex two-tiered network is formed with a simple octahedral metal center, noting the $[Mn_3(\mu_3\text{-}F)]$ cluster had a slight pyramidal aspect to it, a structural feature which is considerably enhanced in L1. A simple **kgd** network has been reported with the ligand acting as the 6-connecting center,[31] and other examples include decorated **kgd** nets where the 6-connecting node is a dinuclear,[32] or trinuclear metal cluster.[33]

2.2.2. 3-Connected Coordination Polymers. The 3,6-connected coordination networks of **1**−**4** employed weakly coordinating anions ClO_4^- or BF_4^-. The use of more strongly coordinating anions may lower the connectivity of any metal-based node within a coordination polymer. This effect is seen in complexes $\{[Cd(L3)(NO_3)_2]\cdot 2(DMF)\}_\infty$ **5**, $\{[Zn(L3)(NO_3)_2]\cdot 2(DMF)\}_\infty$ **6**, and $\{[Cu_5(L3)_2Cl_{10}(NMP)_4]\cdot n(NMP)\}_\infty$ **7**, where the network connectivity of the metal is reduced to three or two due to coordinating anions, resulting in 3-connected coordination polymers of 6^3 (**hcb**) or decorated 6^3 topology. The **hcb** topology is a relatively common 3-connected topology for coordination polymers.[34]

Table 3. Selected Bond Lengths (Å) and Angles (deg) for Complexes 1−4[a]

Complex 1					
Ag1−O4	2.436(5)	O4−Ag1−O4^{i}	180.0(3)	O4−Ag1−Ag2	126.35(11)
Ag1−O4^{i-v}	2.436(5)	O4^{iv}−Ag1−O4^{v}	88.46(16)	O4−Ag1−Ag2^{i}	53.65(11)
Ag2−O5	2.414(6)	O4^{iv}−Ag1−O4	91.54(16)	O5−Ag2−Ag1	119.23(11)
Ag2−O5^{ii}	2.413(6)	O4−Ag1−O4^{ii}	88.46(16)	O5^{ii}−Ag2−O5	98.18(16)
Ag2−O5^{iii}	2.414(6)	O4−Ag1−O4^{iii}	88.46(16)	O5^{iii}−Ag2−O5	98.18(16)
Ag1−Ag2	3.2753(9)	O4−Ag1−O4^{iv}	91.54(16)	O5^{ii}−Ag2−O5^{iii}	98.18(16)
Ag1−Ag2^{i}	3.2753(9)	O4^{v}−Ag1−O4^{ii}	180		
Complex 2					
Zn1−O8^{i-ii}	2.089(4)	O10^{i}−Zn1−O10^{ii}	179.999(2)	O10^{i}−Zn1−O12^{iv}	92.24(17)
Zn1−O10	2.099(4)	O10^{ii}−Zn1−O8^{i}	88.11(19)	O8−Zn1−O12^{iv}	88.44(18)
Zn1−O10^{iii}	2.089(4)	O10^{i}−Zn1−O8	88.11(19)	O8−Zn1−O12^{v}	91.56(18)
Zn1−O12^{iv-v}	2.099(4)	O8^{ii}−Zn1−O8	179.999(2)	O12^{iv}−Zn1−O12^{v}	180.00(18)
Complex 3					
Co1−O12	2.065(4)	O12−Co1−O12^{i}	180.0(2)	O12^{i}−Co1−O8^{v}	89.83(17)
Co1−O12^{i}	2.065(4)	O12−Co1−O10^{ii}	90.5(3)	O10^{ii}−Co1−O10^{iii}	180.00(17)
Co1−O10^{ii-iii}	2.113(5)	O12−Co1−O8^{v}	90.17(17)	O8^{iv}−Co1−O8^{v}	180.0(2)
Co1−O8^{iv-v}	2.051(4)	O12^{i}−Co1−O10^{i}	89.5(3)		
Complex 4					
Cu1−O11	1.978(5)	O11−Cu1−O11^{i}	179.997(2)	O10−Cu2−O21	89.2(2)
Cu1−O11^{i}	1.978(5)	O11^{i}−Cu1−O24^{iv}	87.7(2)	O23^{v}−Cu2−O21	83.1(2)
Cu1−O24^{ii-iii}	2.003(5)	O11−Cu1−O24^{iv}	92.3(2)	O23^{vi}−Cu2−O21	96.9(2)
Cu1−O22	2.435(5)	O11−Cu1−O24^{iii}	87.7	O10^{iv}−Cu2−O21^{iv}	89.2(2)
Cu1−O22^{i}	2.435(5)	O24^{iv}−Cu1−O24^{iii}	179.998(2)	O23^{vi}−Cu2−O21^{iv}	83.1(2)
Cu2−O10	1.976(6)	O11−Cu1−O22^{i}	85.1(2)	O21−Cu2−O21^{iv}	179.999(2)
Cu2−O10^{iv}	1.976(6)	O24^{iv}−Cu1−O22^{i}	90.5(2)	O26−Cu3−O27	169.2(3)
Cu2−O23^{v}	1.984(6)	O24^{iii}−Cu1−O22^{i}	89.5(2)	O26−Cu3−O29	88.8(3)
Cu2−O23^{vi}	1.984(6)	O11−Cu1−O22	94.9(2)	O27−Cu3−O29	87.1(3)
Cu2−O21	2.415(6)	O24^{iv}−Cu1−O22	89.5(2)	O26−Cu3−O25	90.3(2)
Cu2−O21^{iv}	2.415(6)	O22^{i}−Cu1−O22	180.0(2)	O27−Cu3−O25	89.6(3)
Cu3−O25	1.991(7)	O10−Cu2−O10^{v}	179.998(1)	O29−Cu3−O25	157.3(3)
Cu3−O26	1.955(5)	O10−Cu2−O23^{v}	93.1(3)	O26−Cu3−O28	102.2(2)
Cu3−O27	1.962(6)	O10^{iv}−Cu2−O23^{v}	86.9(3)	O27−Cu3−O28	88.5(2)
Cu3−O28	2.193(6)	O10^{iv}−Cu2−O23^{vi}	93.1(3)	O29−Cu3−O28	103.9(3)
Cu3−O29	1.967(9)	O23^{v}−Cu2−O23^{vi}	179.998(2)	O25−Cu3−O28	98.5(3)

[a]Symmetry operations: Complex 1: i 1−*x*, 1−*y*, −*z*; ii 1−*y*, *z* + 1/2, −*x* + 1/2; iii −*z* + 1/2, 1−*x*, *y* − 1/2; iv *z* + 1/2, *x*, −*y* + 1/2; v *y*, −*z* + 1/2, *x* − 1/2. Complex 2: i 1−*x*, 2−*y*, 1−*x*; ii *x*, 1+*y*, *z*; 1−*x*, 1−*y*, *z*; iv −*x*, 2−*y*, 1−*z*; v 1+*x*, 1+*y*, *z*. Complex 3: i −*x* + 1/2, 1−*y* + 1/2, 1−*z*; ii *x* − 1/2, *y* + 1/2, *z*; iii 1−*x*, 1−*y*, 1−*z*; iv 1−*x* + 1/2. 1−*y* + 1/2, 1−*z*; v 1−*x*, *y*, *z*. Complex 4: i 1−*x*, −*y*, 1−*z*; ii 2−*x*, −*y*, 1−*z*; iii 1−*x*, *y*, *z*; iv 2−*x*, 1−*y*, −*z*; v 2*x*, *y*, *z*; vi 1−*x*, 1−*y*, −*z*.

Complexes $\{[Cd(L3)(NO_3)_2]\cdot 2(DMF)\}_\infty$ **5** and $\{[Zn(L3)(NO_3)_2]\cdot 2(DMF)\}_\infty$ **6** are isostructural. Only complex **5** will be discussed in detail, as crystals of **6** were twinned.[35] Complex **5** crystallizes in a monoclinic cell, and the structure was solved in the chiral space group $P2_1$. Selected bond lengths and angles are given in Table 4. The given formula also comprises the asymmetric unit of the structure. The Cd ion is sited on a general position and is coordinated by two chelating nitrate anions and three L2 ligands through the 2-pyridyl-*N*-oxide groups in an approximately trigonal bipyramidal fashion (considering each chelating nitrate as occupying one coordination position), Figure 7a. The three 2-pyridyl-*N*-oxide groups around the Cd(II) are in a T-shaped orientation. The L3 ligand bridges between three symmetry-related Cd ions, thus forming a 2-D network where both the metal ion and the ligand are 3-connecting. The 2-pyridyl-*N*-oxide groups of ligand L3 are linked to the tribenzo[*a*,*d*,*g*]cyclononatriene core via methylene ether linkages, unlike the ester linkage employed in ligands L1 and L2. This gives the side-arms considerably more rotational flexibility, as was also noted for the clathrate structures, and the three 2-pyridyl-*N*-oxide groups of L3 in complex **5** each have quite different orientations with respect to the tribenzo[*a*,*d*,*g*]cyclononatriene core, Figure 7a.

The 2-D coordination network formed is a 3-connected "chicken-wire" network of 6^3 topology, Figure 7b. The L3 ligands within the $[Cd(L3)(NO_3)_2]$ network have alternating cavity-up, cavity-down arrangements, and each ligand within the network is the same enantiomer. Indeed, the overall structure only contains one of the two ligand enantiomers, although the bulk mixture is a racemate. Such self-sorting or spontaneous resolution upon crystallization to form a conglomerate is known for both molecular, host−guest, and network crystalline materials.[36] Packing of the 2-D networks in the crystal lattice occurs with small channels along the *a* axis which are occupied by DMF solvent, Figure 7c.

Complex $\{[Cu_5(L3)_2Cl_{10}(NMP)_4]\cdot n(NMP)\}_\infty$ **7** crystallizes in a triclinic cell, and the asymmetric unit is half of the given formula with three NMP positions located in the difference map. Selected bond lengths and angles are given in Table 4. There are three crystallographically independent Cu(II) ions in **7**, one of which is located on an inversion center. The Cu on an inversion center has square planar geometry with *trans* terminal Cl ligands and *trans* *N*-oxide ligands from two symmetry-

dx.doi.org/10.1021/ic300940k | *Inorg. Chem.* 2012, 51, 10657−10674

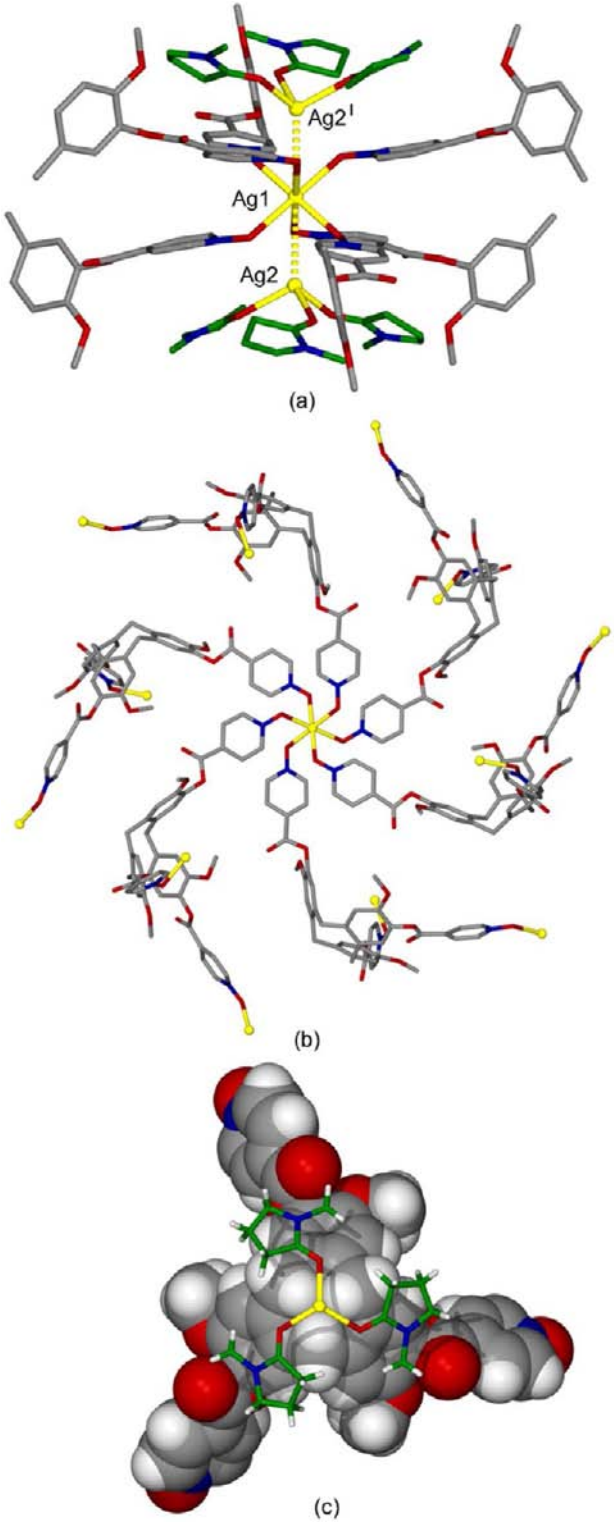

Figure 2. From the crystal structure of $\{[Ag_3(NMP)_6(L1)_2]\cdot 3(ClO_4)\cdot n(NMP)\}_\infty$ **1**. Hydrogen atoms are omitted for clarity. (a) Ag coordination spheres showing linear Ag2···Ag1···Ag2 trimer, with the dashed lines representing argentophilic interactions. NMP ligands are shown in green, and only one-third of each L1 ligand is shown for clarity; (b) six L1 ligands surrounding Ag1 and the 3-connecting behavior of L1, Ag2 ions are not shown; (c) detail showing positioning of one $\{(Ag2)(NMP)_3\}$ moiety and L1 ligand on the same 3-fold axis. Symmetry operation I: $1-x$, $1-y$, $-z$.

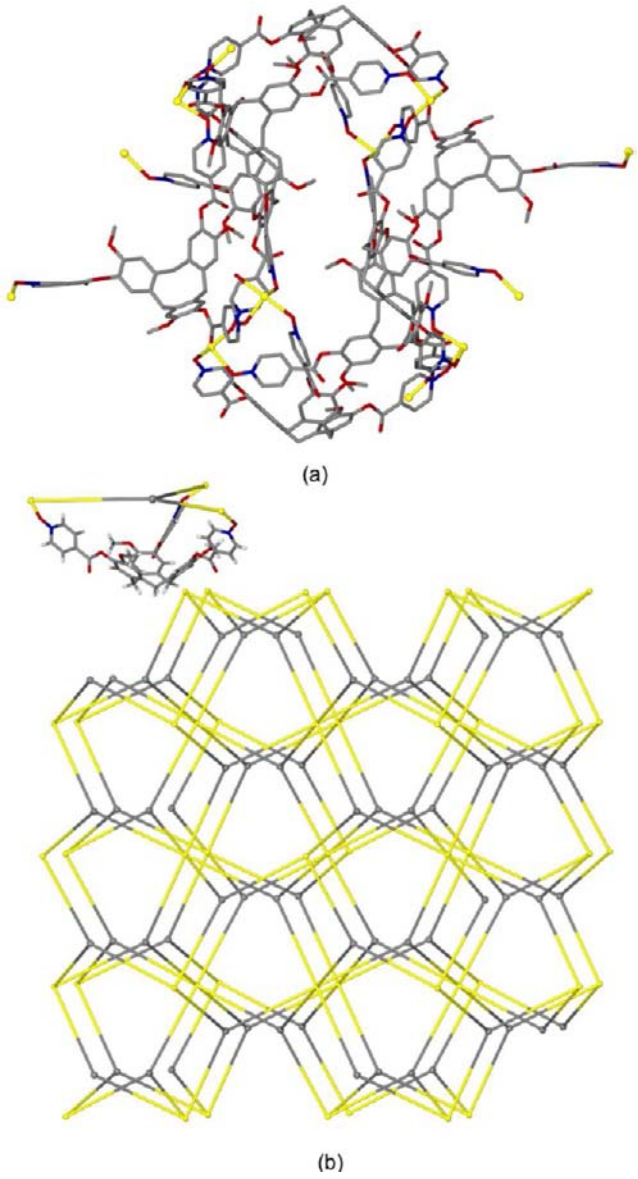

Figure 3. From the crystal structure of **1**, with $\{(Ag2)(NMP)_3\}$ moieties removed for clarity. (a) section of the 3-D coordination polymer, showing formation of large cavities within the framework; (b) connectivity diagram showing **pyr** topology with Ag1 ions in yellow and central ligand position in gray, inset at top left shows positioning of 3-connecting center with respect to the L1 ligand.

related L3 ligands. The other two Cu positions relate to two centrosymmetric dinuclear Cu(II) clusters which are doubly bridged by μ_2-*N*-oxide coordination. Each of the Cu ions in the dinuclear clusters have square planar geometry with two terminal Cl anions in the basal plane, Figure 8a. Similar structural motifs featuring $[Cu_2Cl_4\text{-}\mu_2\text{-}(\text{pyridyl-}N\text{-oxide})_2L_2]$ where L is a terminal ligand have been reported before[37,38] including an example with a bridging bis(pyridyl-*N*-oxide) which forms a coordination chain structure.[38]

$[Cu_5(L3)_2Cl_{10}(NMP)_4]$ forms a 2-D coordination network. There is one crystallographically unique L3 ligand in **7**, and it binds to one mononuclear Cu and to two Cu_2 dimers, thus is a 3-connecting center in the network. Both the mononuclear Cu and Cu_2 dimers are effectively 2-connecting nodes for the network and are thus topologically trivial. The network has a decorated 6^3 topology, Figure 8b. Each L3 ligand within the

dx.doi.org/10.1021/ic300940k | *Inorg. Chem.* 2012, 51, 10657−10674

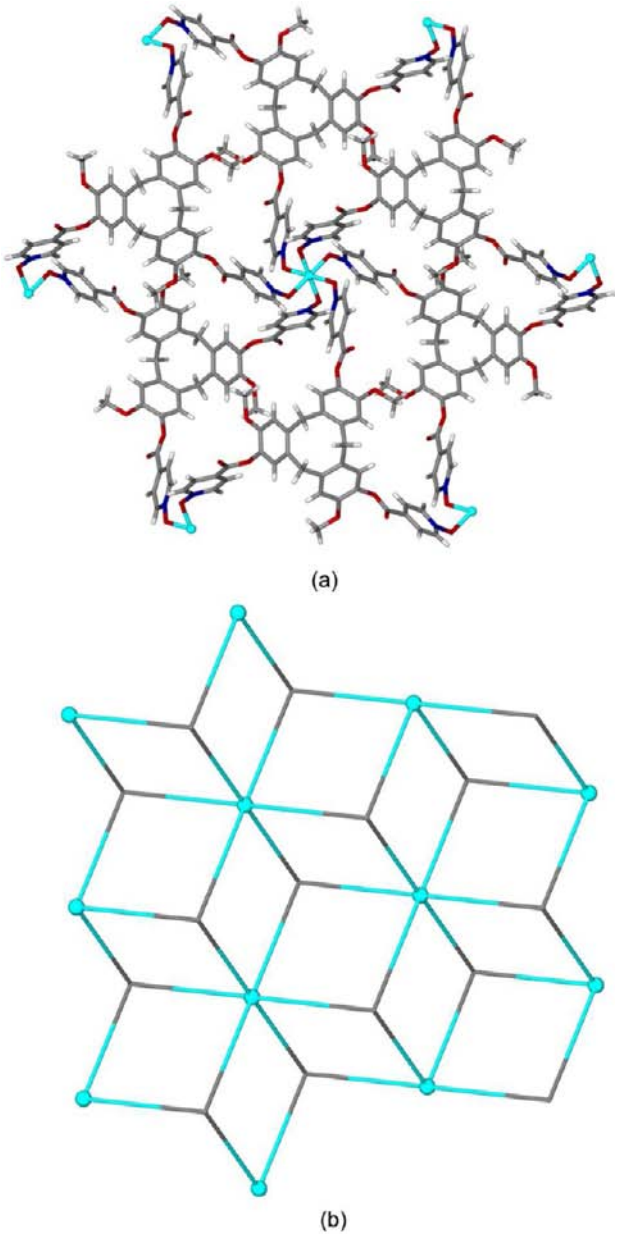

Figure 4. Details from the X-ray structure of $\{[Zn(L1)_2]\cdot 2(BF_4)\cdot n(NMP)\}_\infty$ **2** showing: (a) Zn(II) coordination; (b) connectivity diagram showing **kgd** network, Zn(II) ions as blue spheres, center of ligands in gray.

network is a host for one NMP guest molecule as shown in Figure 8a, with the hydrophobic $-CH_2-$ directed into the hydrophobic cavity. Two other crystallographically independent NMP molecules were located in the crystal structure, one forms the second coordination sphere of the square planar Cu(II), with two symmetry equivalent NMP above and below the plane at Cu···O separation 3.61 Å. The other is approximately aligned with one phenyl ring of L3, sitting about 4 Å above it. Within the crystal lattice, the 2-D $[Cu_5(L3)_2Cl_{10}(NMP)_4]$ coordination polymers have an offset alignment with L3 ligands of one network above metal positions of the adjacent network. This creates a series of large channels that run along the *a* axis, and are approximately 12 × 16 Å in cross-section, Figure 8c. There are likely to be further disordered solvent positions within these channels, which account for around 40% of the unit cell volume. TGA is consistent with 12 solvent NMP molecules per $[Cu_5(L3)_2Cl_{10}(NMP)_4]$, noting 4 of these were found in the crystal structure. Loss of the 12 NMP molecules is stepwise to about 200 °C. The material was not observed to retain crystallinity upon solvent evacuation.

2.2.3. Discrete Complexes and Coordination Polymers with Self-Inclusion Motifs. In each of the coordination polymers described above the ligands L1 or L3 bridge between three metal ions employing each of their pyridyl-*N*-oxide groups; however, this does not always occur. In the discrete complex $[Cu(L1)Cl_2(DMF)_2]\cdot 2(H_4O)$ **8** only one 4-pyridyl-*N*-oxide group is engaged in metal complexation, while in $[Ag_2(L3)_2(NMP)_4]\cdot 2(BF_4)\cdot 2(NMP)$ **9** only two 2-pyridyl-*N*-oxide groups bind to Ag(I) cations. Furthermore in all of the complexes that were isolated with ligand L2 only two of the three 3-pyridyl-*N*-oxide groups complex to metal cations. These complexes are $\{[Cd(L2)_2(DMF)_2]\cdot 2ClO_4\cdot 8(DMF)\}_\infty$ **10**, $\{[Cu(L2)_2(DMF)_2]\cdot 2ClO_4\cdot 8(DMF)\}_\infty$ **11**, and $\{[Co(L2)_2(DMF)_2]\cdot 2NO_3\cdot 4(DMF)\cdot H_2O\}_\infty$ **12**. An apparent trend is that in complexes where there are pyridyl-*N*-oxide groups that do not bind to a metal cation, then there are also self-inclusion motifs either between or within the complexes.

The mononuclear species $[Cu(L1)Cl_2(DMF)_2]\cdot 2(H_4O)$ **8** was initially formed from a 1:1 mixture of $CuCl_2$ and L1. Use of different stoichiometries did not result in a different complex being isolated. Complex **8** crystallizes with a triclinic unit cell, and there is one formula unit in the asymmetric unit. ESI-MS also shows a 1:1 Cu(I):L1 complex. The Cu(II) ion has a distorted five-coordinate geometry, Figure 9a, with selected bond lengths and angles given in Table 5. The largest angles are O−Cu−O of 171.9(6) and Cl−Cu−Cl of 148.35(16)°, giving a τ of about 0.4 which is closer to a square pyramidal geometry than trigonal bipyramidal.[26] There is a DMF ligand in the apical site and *trans* Cl^- ligands in the basal plane, and one *N*-oxide ligand and a further DMF ligand. The L1 ligand coordinates through the one *N*-oxide group to give a discrete complex; however, a network of different supramolecular interactions form throughout the crystal lattice. A chain of $[Cu(L1)Cl_2(DMF)_2]$ complexes form through host−guest interactions between individual units where the apically coordinated DMF ligand acts as a guest molecule, with one of its methyl groups being directed into the hydrophobic cavity of the L1 ligand of an adjacent complex, Figure 9b. Association or network formation through interspecies self-complementary host−guest interactions has been previously observed with CTV-type ligands.[9,10] The host−guest chains are linked into a 2-D network in the *ab* plane through face-to-face $\pi-\pi$ stacking interactions that occur between one of the uncomplexed pyridyl-*N*-oxide moieties and its inverted symmetry equivalent of an adjacent complex, Figure 9c. The ring centroid separations are 3.53 Å.

The discrete complex $[Ag_2(L3)_2(NMP)_4]\cdot 2(BF_4)\cdot 2(NMP)$ **9** also features a self-inclusion motif; however in this case it is a further example of the hand-shake motif, similar to that described in section 2.1 for the clathrate L2·2(NMP). In **9** the hand-shake motif occurs within the $[Ag_2L_2]$ assembly, Figure 10. The structure of **9** was solved in the monoclinic space group $P2_1/c$. The cationic complex $[Ag_2(L3)_2(NMP)_4]^{2+}$ is a discrete dimer, and the asymmetric unit of the crystal structure is half the given composition as the dimer is centrosymmetric. The Ag(I) within $[Ag_2(L3)_2(NMP)_4]^{2+}$ is on a general position and has distorted 4-coordinate geometry being coordinated by two 2-pyridyl-*N*-oxide groups from two symmetry equivalent L3

dx.doi.org/10.1021/ic300940k | *Inorg. Chem.* 2012, 51, 10657−10674

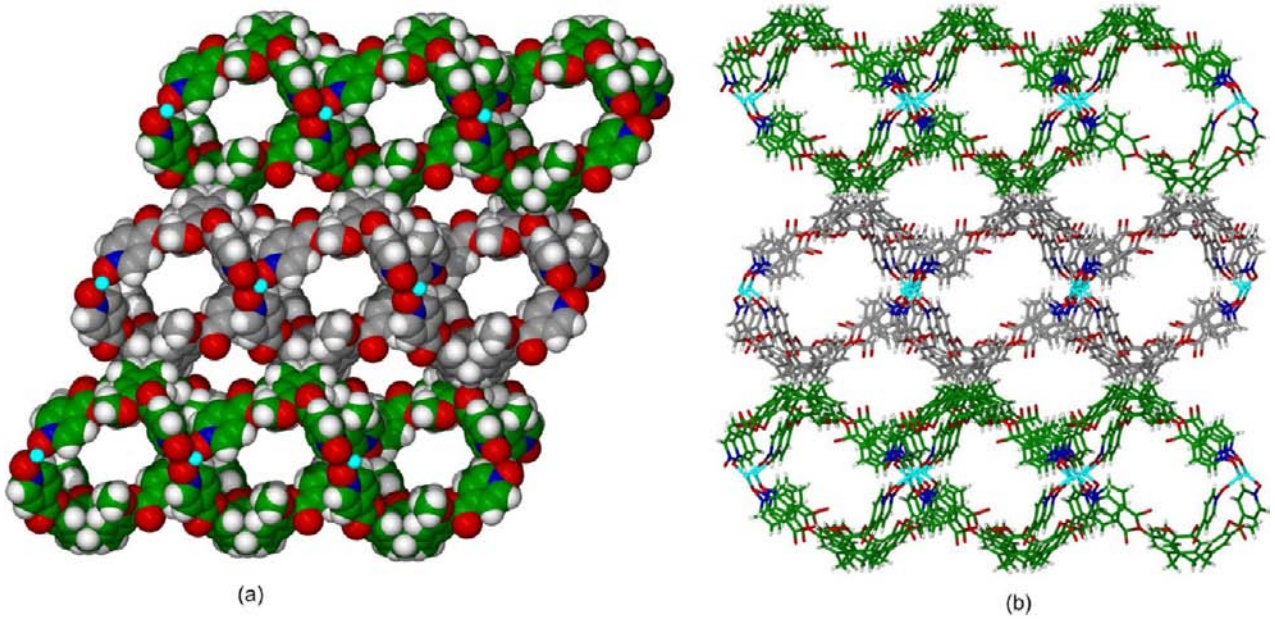

Figure 5. Packing diagrams of $\{[Zn(L1)_2]\cdot 2(BF_4)\cdot n(NMP)\}_\infty$ **2** and$\{[Co(L1)_2]\cdot 2(BF_4)\cdot n(DMF)\}_\infty$ **3** (a) complex **2** viewed down the *b* axis; and (b) complex **3** viewed down the *a* axis. Different 2-D coordination polymers are distinguished by color.

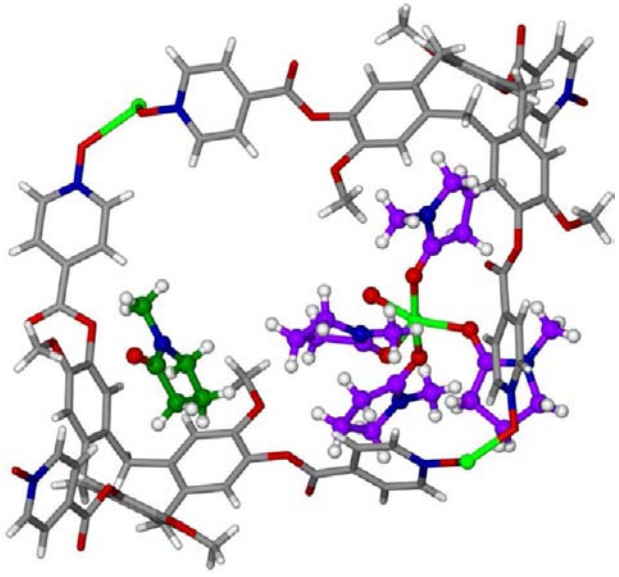

Figure 6. Detail from the crystal structure of complex $\{[Cu(L1)_2]\cdot[Cu(H_2O)(NMP)_4]\cdot 4(BF_4)\cdot 8(NMP)\cdot 2(H_2O)\}_\infty$ **4** highlighting the host–guest interactions between ligand L1 and NMP (shown in green) and ligand L1 and $[Cu(H_2O)(NMP)_4]^{2+}$ cation (shown in purple).

ligands and two NMP solvent molecules, Table 5. Each L3 ligand coordinates to two Ag(I) ions and one 2-pyridyl-*N*-oxide group remains uncoordinated. Within the $[Ag_2L_2]$ assembly, one of the coordinating 2-pyridyl-*N*-oxide moieties occupies the guest position of the molecular cavity of the second L3 ligand and vice versa. $\pi-\pi$ stacking interactions are apparent with a face-to-face interaction between the pyridyl-*N*-oxide and one phenyl ring of the tribenzo[*a*,*d*,*g*]cyclononatriene core at a ring centroid separation of 3.78 Å, and edge-to-face interaction at C–H···ring centroid distance 2.67 Å, Figure.10a. Electrospray mass spectrometry of a NMP solution of a 1:1 mixture of $AgBF_4$ and L3 indicates that the complex is also present in solution, although loses its more weakly bound NMP ligands before detection. The peak observed at *m*/*z* of 1760.97 corresponds to species $\{[Ag_2(L3)_2]\cdot BF_4\}^+$, and a peak corresponding to $\{Ag(L3)\}^+$ was also observed.

Within the crystal lattice there are multiple face-to-face $\pi-\pi$ stacking interactions between the $[Ag_2(L3)_2(NMP)_4]^{2+}$ complexes. The intercomplex face-to-face $\pi-\pi$ stacking interactions formed by one complex are shown in Figure 10b. Each $[Ag_2(L3)_2(NMP)_4]^{2+}$ complex forms such interactions to four other complexes. These occur between the uncomplexed 2-pyridyl-*N*-oxide groups and the phenyl rings of an adjacent complex (ring centroid separation 3.55 Å) and the guest complexed 2-pyridyl-*N*-oxide groups with phenyl rings of an adjacent complex (ring centroid separation 3.61 Å).

Complexes $\{[Cd(L2)_2(DMF)_2]\cdot 2ClO_4\cdot 8(DMF)\}_\infty$ **10** and $\{[Cu(L2)_2(DMF)_2]\cdot 2ClO_4\cdot 8(DMF)\}_\infty$ **11** are isostructural, and feature 2-D $\{[M(L2)_2(DMF)_2]^{2+}$ coordination polymers. Only complex **10** will be discussed in detail, and selected bond lengths and angles for both complexes are given in Table 5. Complex **10** crystallizes with a monoclinic unit cell, and the asymmetric unit is half the given composition. The Cd(II) cation is positioned on an inversion center, and has approximately octahedral coordination geometry. There are two symmetry equivalent DMF ligands in a *trans* arrangement and a square planar arrangement of four 3-pyridyl-*N*-oxide ligands from four symmetry-related L2 ligands, Figure.11a. The coordination sphere of the analogous Cu(II) species **11** shows the anticipated Jahn–Teller elongations, Table 5. The 3-pyridyl-*N*-oxide derived L2 only coordinates through two of its three 3-pyridyl-*N*-oxide groups, thus forming a topologically trivial 2-connecting node within the coordination polymer. The $[Cd(L2)_2(DMF)_2]^{2+}$ coordination polymer has a 4^4 (**sql**) grid structure with only the Cd ions acting as topological connecting nodes, Figure 11b. The **sql** topology is commonly observed for 4-connected coordination polymers.[39]

The uncomplexed 3-pyridyl-*N*-oxide of each L2 ligand within the network acts as the intracavity guest for a second L2 ligand within the network, in a further example of the hand-shake

Table 4. Selected Bond Lengths (Å) and Angles (deg) for Complexes 5–7[a]

Complex 5					
Cd1–O7	2.255(4)	O7–Cd1–O8^{i}	91.32(14)	O8^{i}–Cd1–O11	90.86(16)
Cd1–O8^{i}	2.252(4)	O7–Cd1–O9^{i}	89.73(14)	O8^{i}–Cd1–O12	100.04(17)
Cd1–O9^{ii}	2.283(4)	O8^{i}–Cd1–O9^{ii}	174.43(14)	O9^{ii}–Cd1–O11	92.10(16)
Cd1–O11	2.444(5)	O7–Cd1–O11	137.08(17)	O9^{ii}–Cd1–O12	85.51(16)
Cd1–O12	2.454(5)	O7–Cd1–O12	84.78(17)		
Cd1–O14	2.456(5)	O7–Cd1–O14	89.25(14)		
Cd1–O15	2.390(4)	O7–Cd1–O15	142.55(15)		
Complex 7					
Cu1–O7	2.002(2)	O7–Cu1–O7^{i}	70.48(10)	O9–Cu3–Cl5	161.28(9)
Cu1–O7^{i}	2.046(2)	O7–Cu1–O10	86.05(9)	O9–Cu3–O12^{iv}	87.94(13)
Cu1–Cl1	2.2200(10)	O7–Cu1–Cl1	93.29(7)	Cl4–Cu3–Cl5	100.78(5)
Cu1–Cl2	2.2175(9)	O7–Cu1–Cl2	162.17(7)	O9^{iii}–Cu3–Cl4	160.00(10)
Cu1–O10	2.336(2)	Cl1–Cu1–Cl2	100.16	O9^{iii}–Cu3–Cl5	93.94(10)
Cu2–O8	1.962(3)	O7^{i}–Cu1–Cl1	156.45(7)	O9^{iii}–Cu3–O12^{iv}	86.84(12)
Cu2–O8^{ii}	1.962(3)	O7^{i}–Cu1–Cl2	93.05(7)		
Cu2–Cl3	2.2524(10)	O7^{i}–Cu1–O10	91.29(9)		
Cu2–Cl3^{ii}	2.2524(10)	O8–Cu2–O8^{ii}	180.0		
Cu3–O9	2.033(3)	O8–Cu2–Cl3	93.74(8)		
Cu3–O9^{iii}	2.000(3)	Cl3–Cu2–Cl3^{ii}	180.0		
Cu3–Cl4	2.2173(12)	O8^{ii}–Cu2–Cl3	86.26(8)		
Cu3–Cl5	2.2199(16)	O9–Cu3–O9^{iii}	69.98(14)		
Cu3–O12	2.310(4)	O9–Cu3–Cl4	92.98(14)		

[a]Symmetry operations: Complex 5: i 1−*x*, *y* + 1/2, 1−*z*; ii 1−*x*, *y* + 1/2, −*z*. Complex 7: i 1−*x*, 1−*y*, −*z*; ii −*x* − 1, −*y*, −*z*; iii −*x*, 1−*y*, 1−*z*; iv *x*−1, *y*, *z*.

mutual pairwise self-inclusion motif. As for L2·2NMP and complex **9**, in complex **10** there are face-to-face $\pi-\pi$ stacking interactions between the guest pyridyl-*N*-oxide and one of the phenyl rings of the core of the host ligand, with a ring centroid separation of 3.57 Å, Figure 11c. The formation of the hand-shake motif within this 2-D coordination polymer means that there are no significant channels within the 2-D network itself. Cavities are formed by the packing of the 2-D networks, and these are occupied by well-ordered perchlorate anions and DMF solvent (see Supporting Information).

Complex $\{[Co(L2)_2(DMF)_2]\cdot 2NO_3\cdot 4(DMF)\cdot H_2O\}_\infty$ **12** crystallized with a triclinic cell; however, crystals were small and weakly diffracting, and X-ray diffraction data were collected using synchrotron radiation. The asymmetric unit is half the stated composition, and the Co(II) cation is located on an inversion center. The Co(II) coordination environment is very similar to the metal coordination environments of complexes **10** and **11** with two *trans* terminal DMF ligands and four symmetry-related L2 ligands. The geometry is slightly distorted from octahedral; selected bond lengths and angles are given in Table 5.

As for complexes **10** and **11**, the L2 ligand only coordinates to a metal center through two of its three *N*-oxide groups; however, unlike in those examples, a doubly bridged chain structure is formed, Figure 12a. There are two inverted orientations of the L2 ligands within the chain, with the molecular cavity directed either up or down. Again, in keeping with the host–guest associations found for **10** and **11**, the uncomplexed 3-pyridyl-*N*-oxide group of each L2 acts as an intracavity guest for an adjacent L2 host ligand, and the association once again forms in a self-complementary hand-shake motif, Figure 12b. On this occasion however, the hand-shake motif occurs in an interchain manner rather than the intranetwork association seen in **10** and **11**. Face-to-face $\pi-\pi$ stacking interactions are evident between the guest 3-pyridyl-*N*-oxide and one phenyl ring of the host at a ring centroid separation of 3.64 Å. The 1-D chains therefore associate into a 2-D network through these host–guest interactions. The crystal lattice also contains additional DMF and water solvate, alongside nitrate counter-anions, but these do not form any strong supramolecular associations with neither the coordination chains nor one another (see Supporting Information).

Intranetwork hand-shake interactions involving coordination polymers of CTV-type ligands have been previously reported in ladder-like 3-connected coordination chains.[9,10] The CTV-type ligands involved featured imidazole or phenyl-pyridyl side arm functionality, and in the case of the latter, distances between the guest phenyl and the host phenyl groups were consistent with weak $\pi-\pi$ stacking (ring centroid separation about 3.8 Å).[10] There is also an example of internetwork hand-shake inclusion motif for a 2-D network of a phenyl-pyridyl-derived CTV ligand; however, in that case there was no evidence of any π-stacking.[10] With L2, the only complexes obtained, whether coordination polymers or ligand solvates, formed the hand-shake inclusion motif with strong face-to-face $\pi-\pi$ stacking between the electron deficient 3-pyridyl-*N*-oxide aromatic ring and the electron rich core phenyl ring.

EXPERIMENTAL SECTION

Tris(isonicotinoyl)cyclotriguaiacylene,[8] tris(nicotinoyl)-cyclotriguaiacylene,[14] tris(2-pyridylmethyl)cyclotriguaiacylene,[14] and tris(3-pyridylmethyl)cyclotriguaiacylene,[15] were synthesized according to literature methods. All chemicals were obtained from commercial sources and were used without further purification. NMR spectra were recorded by automated procedures on a Bruker DPX 500 or 300 MHz NMR spectrometer. Electrospray mass spectra (ES-MS) were measured on a Bruker MicroTOF-Q instrument in positive ion mode. Infrared spectra were recorded as solid phase samples on a Perkin-Elmer Spectrometer. Elemental analyses were performed on material that had been washed with diethyl ether, subsequently dried at 80–90 °C under vacuum and then exposed to the atmosphere,

dx.doi.org/10.1021/ic300940k | Inorg. Chem. 2012, 51, 10657–10674

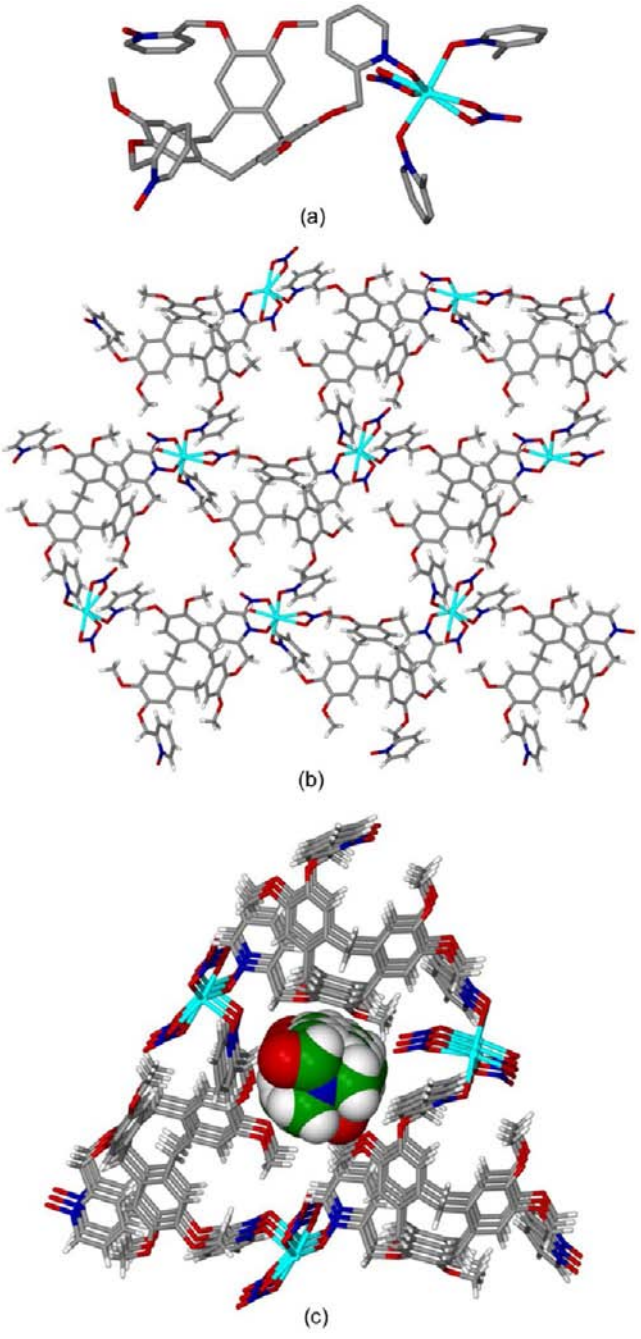

Figure 7. From the crystal structure of $\{[Cd(L3)(NO_3)_2]\cdot 2(DMF)\}_\infty$ **5**. (a) Cd coordination environment; (b) 6^3 network; (c) packing of networks to form DMF (space-filling) filled channels.

hence may show different levels of solvation to those established by crystallography or TGA due to solvent loss and/or absorption of atmospheric water.

Caution! *Although we experienced no problems, perchlorate salts are known to be shock sensitive and should be handled with due care.*

Synthesis. *(±)-2,7,12-Trimethoxy-3,8,13-tris(4-N-oxide-pyridyloxy)-10,15-dihydro-5H-tribenzo[a,d,g]cyclononatriene L1.* Tris(isonicotinoyl)cyclotriguaiacylene (100 mg, 0.138 mmol) was dissolved in dichloromethane (20 mL), and stirred under an argon atmosphere at −78 °C. *m*-CPBA (96 mg, 0.552 mmol) was added to the reaction mixture, and stirred at −78 °C for an hour, followed by 24 h at room temperature, during which time the reaction mixture turned yellow. The reaction was quenched with sat. sodium bicarbonate (3 × 65 mL), and washed with water (50 mL) and brine (50 mL), dried over $MgSO_4$ and concentrated in vacuo. The resultant yellow oily solid was triturated in ethanol to afford a fine off-white solid. Yield 61 mg: 57%; M.pt >300 °C; HR MS (ES^+): *m*/*z* 772.2137 (MH^+); calculated for $C_{42}H_{33}N_3O_{12}$ 771.2059; ^1H NMR (500 MHz, $CDCl_3$) δ (ppm) = 3.69 (d, 3H, endo-C$\underline{H}_2$, *J* = 13.7 Hz), 3.80 (s, 9H, OC$\underline{H}_3$), 4.84 (d, 3H, exo-C$\underline{H}_2$, *J* = 13.7 Hz), 6.94 (s, 3H, aryl-$\underline{H}$), 7.16 (s, 3H, aryl-$\underline{H}$), 8.01 (d, 6H, Py-$\underline{H}^3$, $\underline{H}^5$, *J* = 7.7 Hz), 8.27 (d, 6H, Py-$\underline{H}^2$, $\underline{H}^6$, *J* = 7.7 Hz); $^{13}C\{^1H\}$ NMR (75 MHz, $CDCl_3$) δ (ppm) = 161.9, 149.6, 140.1, 139.2, 137.9, 132.3, 127.4, 124.4, 124.4, 114.9, 56.6, 35.4; Analysis for $C_{42}H_{33}N_3O_{12}\cdot(H_2O)_{0.5}$ (% calculated, found) C (64.61, 64.30), H (4.39, 4.35), N (5.38, 5.30). Infrared (FT-IR, cm^{-1}) 3117 (C−H), 2936 (weak, aromatic C═C−H), 1738 (s, O-C═O), 1612 (m, aromatic C═N), 1506 (s, aromatic C═C), 1478 (s b, aromatic N−O), 1399 (m, aromatic N−O)

(±)-2,7,12-Trimethoxy-3,8,13-tris(3-N-oxide-pyridyloxy)-10,15-dihydro-5H-tribenzo[a,d,g]cyclononatriene L2. Tris(nicotinoyl)-cyclotriguaiacylene (500 mg, 0.690 mmol) was dissolved in dichloromethane (120 mL), and stirred under an argon atmosphere at −78 °C. *m*-CPBA (600 mg, 2.75 mmol) was added to the reaction mixture, and stirred at −78 °C for two hours, followed by 48 h at room temperature. The reaction was quenched with sodium metabisulfite (spatula tip), and washed with sat. aq sodium bicarbonate (2 × 200 mL) and brine (200 mL), dried over $MgSO_4$ and concentrated in vacuo. The resultant off-white solid was triturated in methanol, affording L2 as a bright white solid. Yield 514 mg: 97%; M.pt >270 °C; HR MS (ES^+): *m*/*z* 772.2137 (MH^+); calculated for $C_{42}H_{33}N_3O_{12}$ 771.2059; ^1H NMR (500 MHz, d_6-DMSO) δ (ppm) = 3.71 (d, 3H, endo-C$\underline{H}_2$, *J* = 13.5 Hz), 3.75 (s, 9H, OC$\underline{H}_3$), 4.90 (d, 3H, exo-C$\underline{H}_2$, *J* = 13.5 Hz), 7.32 (s, 3H, aryl-$\underline{H}$), 7.57 (s, 3H, aryl-$\underline{H}$), 7.63 (dd, 3H, Py-$\underline{H}^5$, *J* = 6.36, 7.95 Hz), 7.93 (d, 3H, Py-$\underline{H}^4$, *J* = 8.34 Hz), 8.53 (d, 3H, Py-$\underline{H}^6$, *J* = 6.8 Hz), 8.67 (s, 3H, Py-$\underline{H}^2$); $^{13}C\{^1H\}$ NMR (75 MHz, $CDCl_3$) δ (ppm) = 161.4, 149.4, 143.3, 139.5, 139.3, 137.7, 132.2, 128.9, 127.5, 126.2, 124.3, 114.9, 56.7, 35.3; Analysis for $C_{42}H_{33}N_3O_{12}\cdot 0.5(H_2O)$ (% calculated, found) C (64.61, 64.45), H (4.39, 4.60), N (5.38, 5.30). Infrared (FT-IR, cm^{-1}) 3346 (broad), 2986 (weak, aromatic C═C−H), 1737 (s, O-C═O), 1611 (m, aromatic C═N), 1508 (s, aromatic C═C), 1482 (s b, aromatic N−O), 1435, 1397 (m, aromatic N−O), 1293, 1213, 1133, 1018, 966, 928, 887, 833, 742, 664, 562.

(±)-2,7,12-Trimethoxy-3,8,13-tris(2-N-oxide-pyridylmethoxy)-10,15-dihydro-5H- tribenzo[a,d,g]cyclononatriene L3. Tris(2-pyridylmethyl)cyclotriguaiacylene (250 mg, 0.367 mmol) was dissolved in dichloromethane (50 mL). *m*-CPBA (380 mg, 2.2 mmol) was added to the reaction mixture at −78 °C. After 24 h, sodium hydrogen carbonate was added to quench the reaction. The organic layer was removed, washed with water (2 × 75 mL) and potassium carbonate (2 × 50 mL), dried over $MgSO_4$ and solvent removed in vacuo. The resulting crude solid was purified by recrystallization in acetone (50 mL) and diethyl ether (30 mL), where pure-white crystals of L3 were obtained after 48 h. Yield 110 mg: 41.1%. M.pt 142−145 °C; HR MS (ES^+): *m*/*z* 730.2759 (MH^+); calculated for $C_{42}H_{39}N_3O_9$ 729.2680; ^1H NMR (500 MHz, d_6-DMSO) δ (ppm) = 3.54 (d, 3H, endo-C$\underline{H}_2$, *J* = 13.7 Hz), 3.67 (s, 9H, OC$\underline{H}_3$), 4.68 (d, 3H, exo-C$\underline{H}_2$, *J* = 13.7 Hz), 5.22 (m, 6H, O−C$\underline{H}_2$), 7.08 (s, 3H, aryl-$\underline{H}$), 7.23 (s, 3H, aryl-$\underline{H}$), 7.36 (t, 3H, Py-$\underline{H}^4$, *J* = 7.69 Hz), 7.42 (t, 3H, Py-$\underline{H}^5$, *J* = 7.69 Hz), 7.48 (d, 3H, Py-$\underline{H}^3$, *J* = 7.69 Hz), 8.34 (d, 3H, Py-$\underline{H}^6$, *J* = 5.98 Hz); $^{13}C\{^1H\}$ NMR (75 MHz, $CDCl_3$) δ (ppm) = 147.8, 147.6, 145.9, 139.3, 133.6, 132.3, 125.7, 125.3, 123.9, 115.6, 114.3, 65.2, 56.2, 35.2; Analysis for $C_{42}H_{40}N_3O_9\cdot(H_2O)_{1.5}$ (% calculated, found) C (66.66, 66.95), H (5.59, 5.55), N (5.55, 5.40). Infrared (FT-IR, cm^{-1}) 3107 (C−H), 2920 (weak, aromatic C═C−H), 1643 (m, aromatic C═N), 1585 (s, aromatic C═C), 1518 (s b, aromatic N−O), 1334 (m, aromatic N−O).

(±)-2,7,12-Trimethoxy-3,8,13-tris(3-N-oxide-pyridylmethoxy)-10,15-dihydro-5H-tribenzo[a,d,g]cyclononane L4. Tris(3-pyridylmethyl)cyclotriguaiacylene (150 mg, 0.22 mmol) was dissolved in dichloromethane (∼ 20 mL). *m*-CPBA (227 mg, 1.32 mmol) was added to the reaction mixture at −78 °C. After 1 h, sodium carbonate was added to quench the reaction. The organic layer was removed, washed with water (2 × 50 mL), and the solvent removed in vacuo.

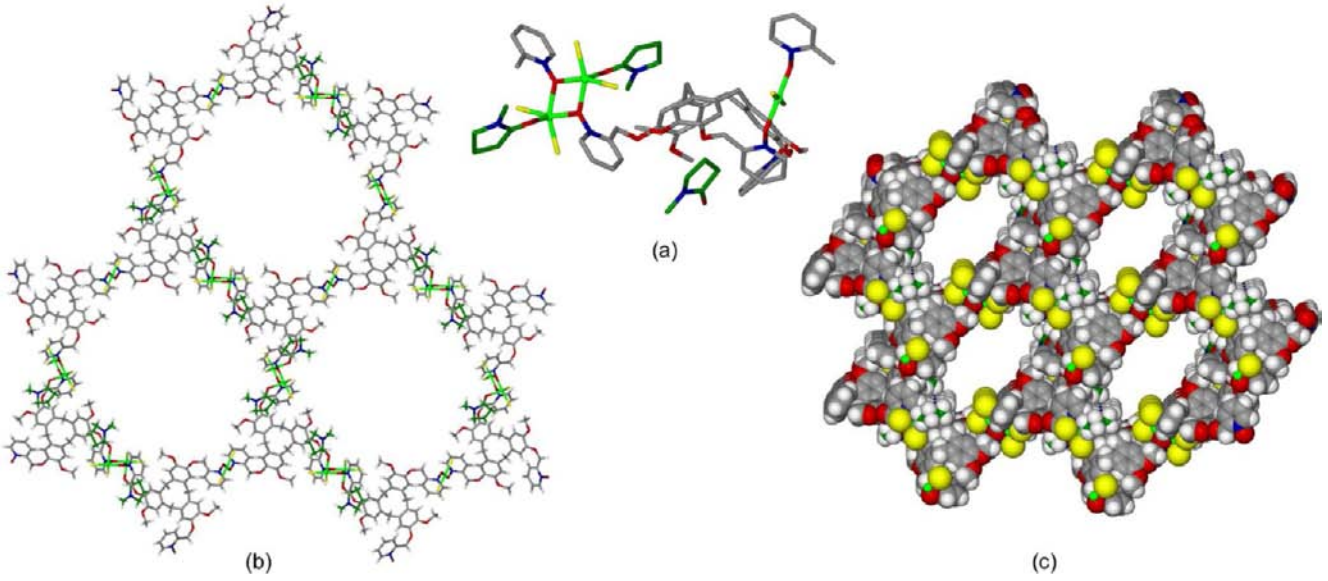

Figure 8. From the crystal structure of $\{[Cu_5(L3)_2Cl_{10}(NMP)_4]\cdot n(NMP)\}_\infty$ **7**. (a) Detail showing square planar mononuclear Cu coordination and one of the two dinuclear square pyramidal Cu clusters, along with host−guest interaction between L3 and NMP; (b) 2-D coordination network of decorated 6^3 topology; (c) space-filling packing diagram showing stacking of networks to form channels down the *a* axis. Chlorides shown in yellow, NMP in dark green.

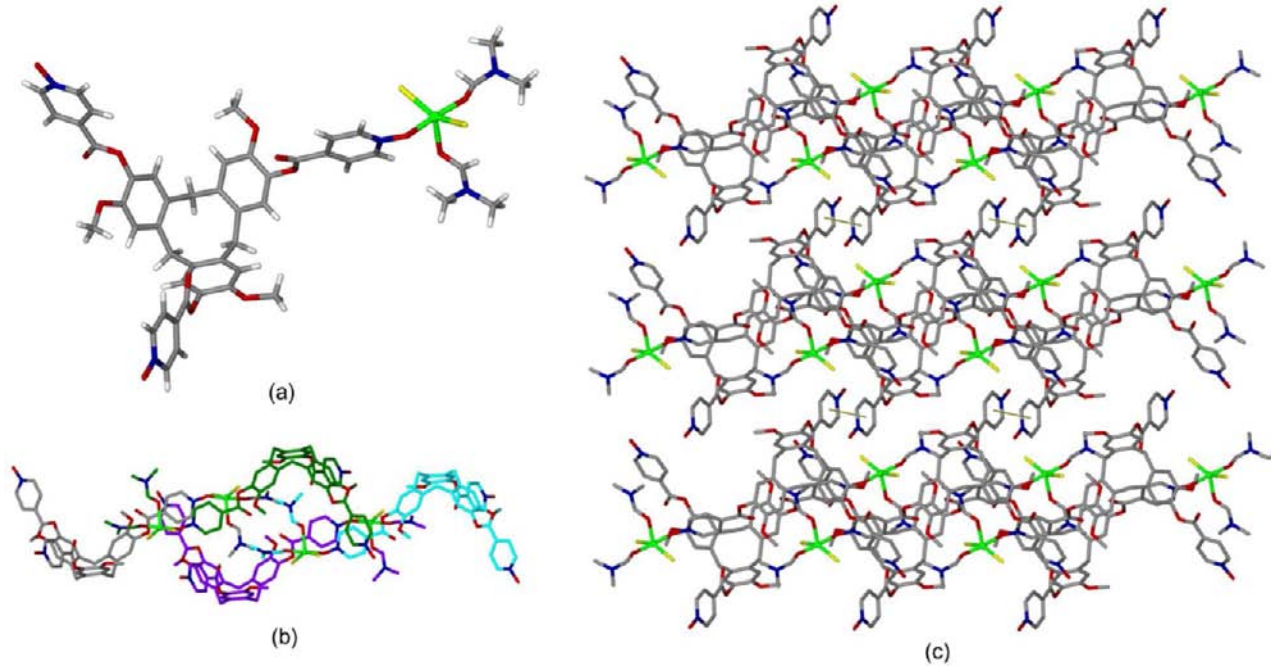

Figure 9. From the crystal structure of **8**. (a) Asymmetric unit showing mononuclear $[Cu(L1)Cl_2(DMF)_2]$; (b) host−guest chain different complexes in different colors; (c) $\pi-\pi$ stacking interactions between the chains (shown as thin lines) to form 2-D network.

The resulting yellow oily solid was triturated in methanol to yield L4 as a yellow powder. Yield 37.6 mg: 25%. HR MS (ES^+): *m*/*z* 730.2756 (MH^+); calculated for $C_{42}H_{39}N_3O_9$ 729.2680; ^1H NMR (500 MHz, CD_2Cl_2) δ (ppm) = 3.48 (d, 3H, endo-C$\underline{H}_2$, *J* = 12.1 Hz), 3.72 (s, 9H, OC$\underline{H}_3$), 4.66 (d, 3H, exo-C$\underline{H}_2$, *J* = 12.2 Hz), 4.95 (m, 6H, O−C$\underline{H}_2$), 6.77 (s, 3H, aryl-$\underline{H}$), 6.84 (s, 3H, aryl-$\underline{H}$), 7.30 (m, 3H, Py-$\underline{H}^5$), 7.47 (d, 3H, Py-$\underline{H}^4$), 7.86 (d, H, Py-$\underline{H}^6$), 7.94 (s, 3H, Py-$\underline{H}^2$); Infrared (FT-IR, cm^{-1}) 3106 (C−$\underline{H}$), 2912 (weak, aromatic C═C−$\underline{H}$), 1658 (m, aromatic C═N), 1559 (s, aromatic C═C), 1521 (s b, aromatic N−O), 1342 (m, aromatic N−O).

General Procedure for Metal Complexes. Crystallization of metal complexes were set up using stock solutions of metal salt and ligand in either NMP or DMF as specified below, and diethyl ether vapors diffused into the solution. Crystals typically formed in 2−3 weeks.

$[Ag_3(NMP)_6(L1)_2]\cdot 3(ClO_4)\cdot n(NMP)$ **1**. $AgClO_4\cdot H_2O$ (5.0 mg, 0.0225 mmol) and L1 (5.0 mg, 0.0075 mmol) in NMP (∼ 2 mL). Yield 9.8 mg. As anticipated, microanalysis indicates a higher level of solvation than refined in the crystal structure, additional solvent added to formula is consistent with analysis of crystal void space and TGA. Microanalysis for $[Ag_3(L1)_2(C_5H_9NO)_6]\cdot 3(ClO_4)\cdot(C_5H_9NO)\cdot 2(H_2O)$ (% calculated, found) C (49.37, 49.30), H (4.63, 5.00), N (6.29, 6.55). Infrared (FT-IR, cm^{-1}) 3463 (broad), 3107, 2938, 1746, 1659, 1510, 1445, 1252, 1166, 1066, 988, 927, 861, 764, 682, 630, 568, 490.

dx.doi.org/10.1021/ic300940k | *Inorg. Chem.* 2012, 51, 10657−10674

Table 5. Selected Bond Lengths (Å) and Angles (deg) for Complexes 8−12[a]

Complex 8					
Cu1−O12	1.974(9)	O12−Cu1−Cl1	92.2(3)	O13−Cu1−O14	86.1(5)
Cu1−O13	2.006(15)	O12−Cu1−Cl2	85.3(3)	O13−Cu1−Cl1	95.7(5)
Cu1−O14	2.212(8)	O12−Cu1−O13	174.9(6)	O13−Cu1−Cl2	87.1(5)
Cu1−Cl1	2.287(4)	O12−Cu1−O14	93.1(4)	O14−Cu1−Cl1	107.0(3)
Cu1−Cl2	2.288(4)	Cl1−Cu1−Cl2	148.35(16)	O14−Cu1−Cl2	104.6(3)
Complex 9					
Ag1−O3	2.224(5)	O3−Ag1−O10	153.3(2)	O10−Ag1−O9^{i}	90.9(3)
Ag1−O10	2.269(7)	O3−Ag1−O11	110.9(4)	O11−Ag1−O9^{i}	87.9(4)
Ag1−O11	2.546(18)	O3−Ag1−O9^{i}	112.3(2)		
Ag1−O9^{i}	2.373(7)	O10−Ag1−O11	81.8(5)		
Complex 10					
Cd1−O8	2.3136(12)	O8−Cd1−O8^{i}	180.00(6)	O10^{ii}−Cd1−O10^{iii}	180.0
Cd1−O8^{i}	2.3137(12)	O8−Cd1−O10^{i}	84.59(4)	O13−Cd1−O13^{i}	180.0
Cd1−O10^{ii-iii}	2.3089(13)	O8−Cd1−O10^{iv}	85.41(4)	O10^{ii}−Cd1−O13	88.86(5)
Cd1−O13	2.2681(11)	O8−Cd1−O13	87.08(4)	O10^{ii}−Cd1−O13^{i}	91.14(5)
Cd1−O13^{i}	2.2681(11)	O8−Cd1−O13^{i}	92.91(4)		
Complex 11					
Cu1−O8^{i-ii}	2.2391(14)	O12−Cu1−O12^{iii}	180.0	O13−Cu1−O13^{iii}	180.0
Cu1−O12	2.3167(13)	O12−Cu1−O8^{ii}	85.34(5)	O8i−Cu1−O8^{ii}	179.998(1)
Cu1−O12^{iii}	2.3167(13)	O12−Cu1−O8^{i}	94.66(5)	O13−Cu1−O8^{ii}	91.90(5)
Cu1−O13	1.9540(11)	O12−Cu1−O13	88.06(5)	O13^{iii}−Cu1−O8^{ii}	88.10(5)
Cu1−O13^{iii}	1.9540(11)	O12−Cu1−O13^{iii}	91.93(5)		
Complex 12					
Co1−O10	2.129(3)	O10−Co1−O10^{i}	179.999(2)	O10−Co1−O11^{ii}	91.04(15)
Co−O10^{i}	2.129(3)	O10−Co1−O13	85.51(14)	O11^{ii}−Co1−O11^{iii}	179.998(2)
Co1−O11^{ii-iii}	2.049(4)	O10−Co1−O13^{i}	94.49(14)	O13^{i}−Co1−O11^{ii}	92.55(16)
Co1−O13	2.094(4)	O13−Co1−O13^{i}	180.0(2)	O13^{i}−Co1−O11^{iii}	87.45(16)
Co1−O13^{i}	2.094(4)	O10−Co1−O11^{iii}	88.95(15)		

[a]Symmetry operations: Complex 9: i 1−*x*, 1−*y*, −*z*. Complex 10: i −*x*, 1−*y*, −*z*; ii −*x* − 1/2, *y* − 1/2, −*z* + 1/2; iii *x* + 1/2, 1−*y* + 1/2, *z* − 1/2. Complex 11: i −*x* − 1/2, *y* + 1/2, 1−*y* + 1/2; ii *x* + 1/2, −*y* + 1/2, *z* − 1/2; iii −*x*, 1−*y*, 1−*z*. Complex 12: i 1−*x*, 2−*y*, 1−*z*; ii 1−*x*, 1−*y*, 1−*z*; iii *x*, 1 + *y*, *z*.

[Zn(L1)$_2$]·2(BF$_4$)·n(NMP) **2**. $Zn(BF_4)_2·6H_2O$ (7.8 mg, 0.0225 mmol) and L1 (5.0 mg, 0.0075 mmol) in NMP (∼ 2 mL). Yield 8.3 mg. Microanalysis for $[Zn(L1)_2]·2(BF_4)·3.5(NMP)·2(H_2O)$(% calculated, found) C (53.11, 52.80), H (5.13, 5.20), N (6.77, 6.90). Infrared (FT-IR, cm^{-1}) 3348 (broad), 1740, 1653, 1619, 1513, 1443, 1402, 1286, 1241, 1170, 1106, 1072, 942, 865, 764, 748, 677, 631.

[Co(L1)$_2$]·2(BF$_4$)·n(DMF) **3**. $Co(BF_4)_2·6H_2O$ (7.6 mg, 0.0225 mmol) and L1 (5.0 mg, 0.0075 mmol) in DMF (∼ 2 mL). Yield 7.1 mg. Analysis for $[Co(L1)_2]·2(BF_4)·4(DMF)·2(H_2O)$ (% calculated, found) C (48.68, 48.70), H (4.92, 4.70), N (7.36, 7.40). Infrared (FT-IR, cm^{-1}) 3333, 2936, 1735, 1634, 1505, 1415, 1254, 1051.

[Cu(L1)$_2$]·[Cu(H$_2$O)(NMP)$_4$]·4(BF$_4$)·8(NMP)·2(H$_2$O) **4**. $Cu(BF_4)_2·4H_2O$ (7.0 mg, 0.0225 mmol) and L1 (5.0 mg, 0.0075 mmol) in NMP (∼ 2 mL). Yield 6.3 mg. Analysis for $[Cu(L1)_2]·2BF_4[Cu(NMP)·4(H_2O)]·2BF_4·5NMP$ (% calculated, found) C (52.92, 52.95), H (5.13, 5.25), N (7.18, 7.20). Infrared (FT-IR, cm^{-1}) 3119, 2938, 1745, 1628, 1505, 1484, 1443, 1404, 1252, 1163, 1139, 1052, 927, 861, 830, 746, 679, 630, 581, 497, 484, 470.

[Cd(L3)(NO$_3$)$_2$]·2(DMF) **5**. $Cd(NO_3)_2·4H_2O$ (7.0 mg, 0.0225 mmol) and L3 (5.0 mg, 0.0075 mmol) in DMF (∼ 2 mL). Yield 7.4 mg. Microanalysis for $[Cd(L3)(NO_3)_2]·2DMF$ (% calculated, found) C (51.12, 51.30), H (4.58, 4.85), N (7.95, 7.50). Infrared (FT-IR, cm^{-1}) 2902, 1674, 1608, 1511, 1441, 1265, 1203, 1150, 1111, 1089, 1050, 1026, 996, 884, 837, 775, 742, 697, 619, 547.

[Zn(L3)(NO$_3$)$_2$]·2(DMF) **6**. $Zn(NO_3)_2·6H_2O$ (6.7 mg, 0.0225 mmol) and L3 (5.1 mg, 0.0075 mmol) in DMF (∼ 2 mL). Yield 11.8 mg. Analysis for $[Zn(L3)(NO_3)_2]$ (% calculated, found) C (54.86, 55.00), H (4.28, 5.50), N (7.62, 8.00). Infrared analysis (FT-IR, cm^{-1}) 3421 (broad), 2928, 1670, 1608, 1511, 1439, 1400, 1262, 1203, 1149, 1088, 1028, 996, 947, 837, 775, 742, 698, 658, 619, 548.

[Cu$_5$(L3)$_2$Cl$_{10}$(NMP)$_4$]·n(NMP) **7**. $CuCl_2·2H_2O$ (3.0 mg, 0.0225 mmol) and L3 (5.0 mg, 0.0075 mmol) in NMP (∼ 2 mL). Yield 8.3 mg. Microanalysis for $[Cu_5(L3)_2(NMP)_4Cl_{10}]·6NMP$ (% calculated, found) C (51.51, 51.10), H (5.42, 5.00), N (7.18, 6.60). Infrared (FT-IR, cm^{-1}) 3310 (broad), 2936, 1633, 1508, 1442, 1398, 1258, 1192, 1148, 1111, 1087, 1046, 993, 843, 781, 743, 694, 658, 619, 556.

[Cu(L1)Cl$_2$(DMF)$_2$]·2(H$_2$O) **8**. $CuCl_2·2H_2O$ (2.6 mg, 0.015 mmol) and L1 (10.1 mg, 0.015 mmol) in DMF (∼ 2 mL). Yield: 7.76 mg. MS (ES$^+$): *m*/*z* 772.2 $[L1H]^+$ (calcd. 772.21), 869.1 $[L1CuCl]^+$ (calcd. 869.10). Analysis for: $[Cu(L1)(DMF)_2Cl_2]·2H_2O$ (% calculated, found) C (52.10, 52.23), H (4.20, 4.37), N (5.80, 5.52). Infrared (FT-IR, cm^{-1}) 3421 (broad), 3509, 3111, 2925, 1733, 1635, 1505, 1440, 1249.

[Ag$_2$(L3)$_2$(NMP)$_4$]·2(BF$_4$)·2(NMP) **9**. $AgBF_4$ (4.3 mg, 0.02 mmol) and L3 (7.5 mg, 0.017 mmol) in NMP (∼ 2 mL). Yield 6.9 mg. MS (ES$^+$): *m*/*z* 1760.97 $\{[Ag_2(L3)_2·BF_4]\}^+$ (calcd. 1760.36), 837.14 $[Ag(L3)]^+$ (calcd. 836.68). Analysis for $[Ag(L3)]·BF_4·H_2O$ (% calculated, found) C (53.52, 53.55), H (4.38, 4.50), N (4.46, 4.55). Infrared analysis (FT-IR, cm^{-1}) 3565 (broad, O−H), 2920 (s, C−H), 1645 (m, C═O), 1607 (m, aromatic C═N), 1515, 1445 (s, aromatic C═C), 1085 (s, b, B−F).

[Cd(L2)$_2$(DMF)$_2$]·2ClO$_4$·8(DMF) **10**. $Cd(ClO_4)_2·6H_2O$ (6.3 mg, 0.015 mmol) and L2 (10.1 mg, 0.015 mmol) in NMP (∼ 2 mL). Yield: 7.76 mg. Microanalysis for: $[Cd(L2)_2(DMF)_2]·2ClO_4·6DMF·2H_2O$ (% calculated, found) C (51.96, 52.15), H (4.63, 4.40), N (6.31, 6.15). Infrared analysis (FT-IR, cm^{-1}) 3421 (broad), 3476, 3104, 2928, 1749, 1667, 1508, 1432, 1283, 1128, 1140, 1094, 1007, 944, 831, 747.

[Cu(L2)$_2$(DMF)$_2$]·2ClO$_4$·8(DMF) **11**. $Cu(ClO_4)_2·6H_2O$ (5.5 mg, 0.015 mmol) and L2 (10.0 mg, 0.015 mmol) in NMP (∼ 2 mL). Yield: 8.41 mg. Microanalysis for: $[Cu(L2)_2(DMF)_2]·2ClO_4·6DMF$ (% calculated, found) C (53.06, 53.00), H (5.28, 5.20), N (8.12, 8.35). Infrared analysis (FT-IR, cm^{-1}) 3421 (broad), 3476, 3104, 2928, 1749, 1667, 1508, 1432, 1283, 1128, 1140, 1094, 1007, 944, 831, 747.

dx.doi.org/10.1021/ic300940k | *Inorg. Chem.* 2012, 51, 10657−10674

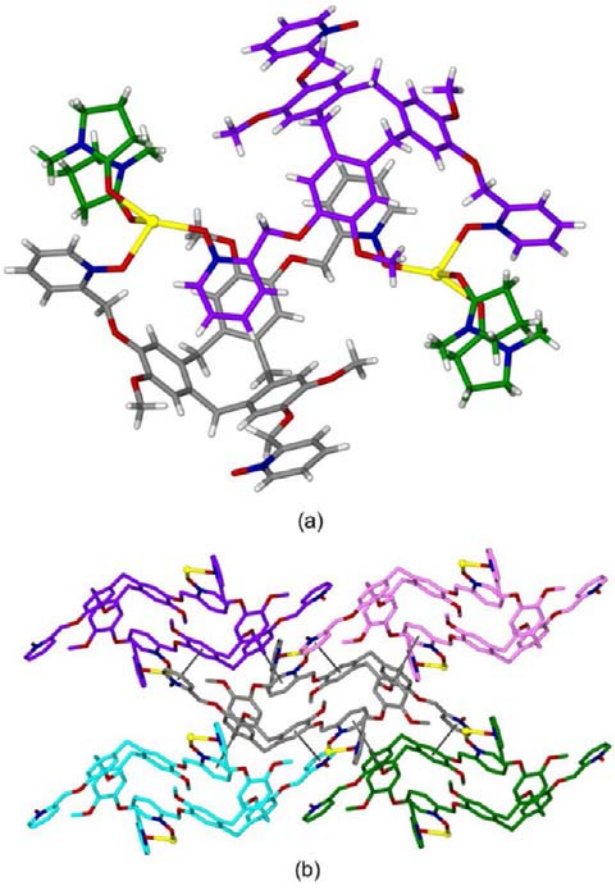

Figure 10. From the crystal structure of $[Ag_2(L3)_2(NMP)_4]\cdot 2(BF_4)\cdot 2(NMP)$ **9**. (a) The hand-shake motif $[Ag_2(L3)_2(NMP)_4]^{2+}$ complex with each L3 ligand shown in a different color; (b) face-to-face $\pi-\pi$ stacking interactions that occur around one $[Ag_2(L3)_2(NMP)_4]^{2+}$ complex shown as thin lines, NMP ligands have been excluded for clarity.

$[Co(L2)_2(DMF)_2]\cdot 2NO_3\cdot 4(DMF)\cdot H_2O$ ***12***. $Co(NO_3)_2\cdot 6H_2O$ (4.2 mg, 0.0146 mmol) and L2 (7.5 mg, 0.0103 mmol) in DMF (~ 2 mL). Yield: 7.76 mg. Microanalysis for: $[Co(L2)_2]\cdot 2NO_3\cdot 3DMF\cdot 4H_2O$ (% calculated, found) C (54.87, 54.90), H (4.80, 4.65), N (7.57, 7.35). Infrared (FT-IR, cm^{-1}) 3402 (broad), 3476, 3044, 2914, 1747, 1648, 1508, 1443, 1375, 1322, 1278 (s), 1202, 1177, 1097, 1003, 939, 829, 742.

X-ray Crystallography. Crystals were mounted under oil on a MiTeGen tip and X-ray diffraction data collected at 150(1) K with Mo-$K\alpha$ radiation (λ = 0.71073 Å) using a Bruker Nonius X-8 diffractometer with ApexII detector and FR591 rotating anode generator, or using synchrotron radiation (λ = 0.6889 Å) with a Rigaku Saturn at station I19 at the Diamond Light Source. Data sets were corrected for absorption using a multiscan method, and structures were solved by direct methods using Superflip,[40] or SHELXS-97 and refined by full-matrix least-squares on F^2 by SHELXL-97,[41] interfaced through the program X-Seed.[42] In general, all non-hydrogen atoms were refined anisotropically and hydrogen atoms were included as invariants at geometrically estimated positions, unless specified otherwise. Details of data collections and structure refinements are given in Tables 1 and 2. Crystallographic data have been deposited with the Cambridge Crystallographic Data Centre as supplementary publications CCDC ########.

L1·DMF was analyzed with synchrotron radiation. The structure of L2·2(NMP) was disordered with one 3-*N*-oxide-pyridyloxy group modeled as disordered over two positions at 60:40 occupancies. This disordered group, along with two NMP solvent molecules, were refined isotropically. Crystals of L3·2(H_2O) were twinned; however,

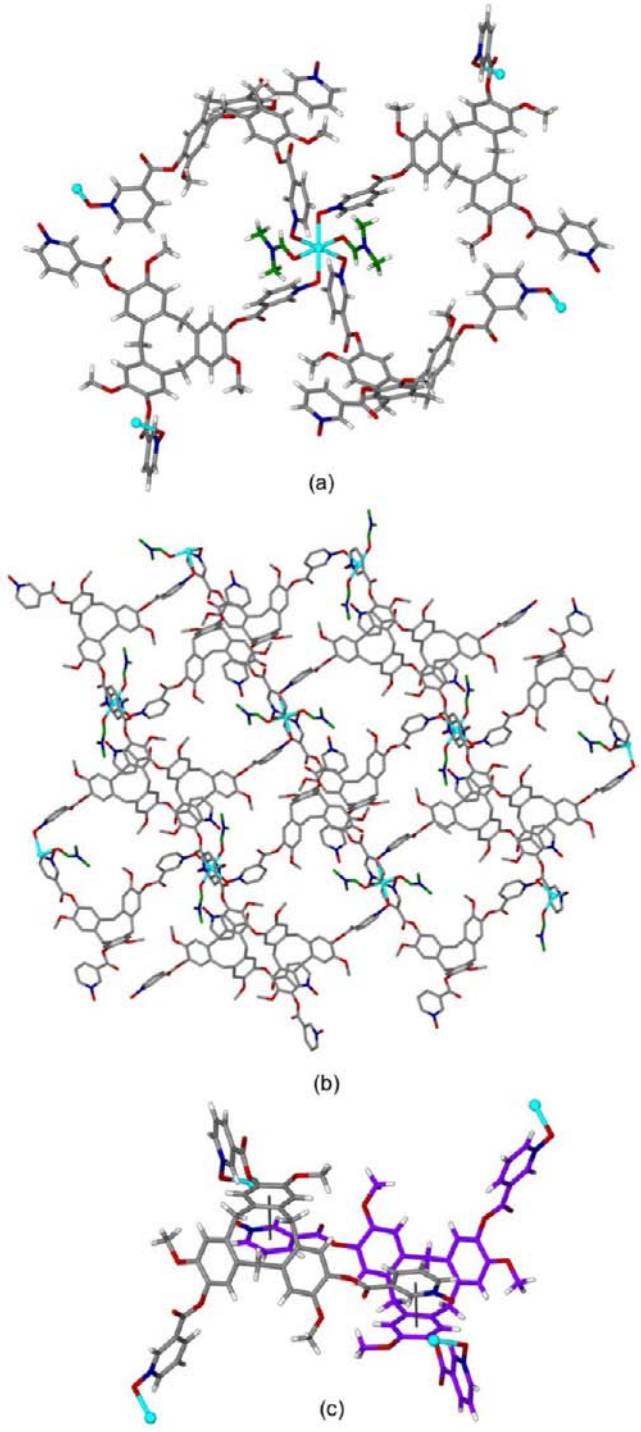

Figure 11. From the crystal structure of $\{[Cd(L2)_2(DMF)_2]\cdot 2ClO_4\cdot 8(DMF)\}_\infty$ **10**. (a) Coordination environment of Cd ion, DMF ligands shown in green; (b) extended diagram of 2-D coordination network, and (c) detail of one hand-shake pair of L1 ligands with $\pi-\pi$ stacking interactions indicated by thin lines.

the data could be refined satisfactorily. Crystals of complexes **2**, **3**, and **8** were weakly diffracting and did not diffract at high angles; hence the structures were refined at lower than ideal resolution. For complexes **1**−**3** and **7** the structures contained significant void space and residual electron density that could not be meaningfully refined as additional solvent; hence the SQUEEZE[43] routine of PLATON[44] was employed. For **3** the aromatic rings were refined with a rigid body model, some bond lengths were restrained and one *N*-oxide-pyridyloxy was refined as disordered. Disordered groups and one methyl were refined

dx.doi.org/10.1021/ic300940k | *Inorg. Chem.* 2012, 51, 10657−10674

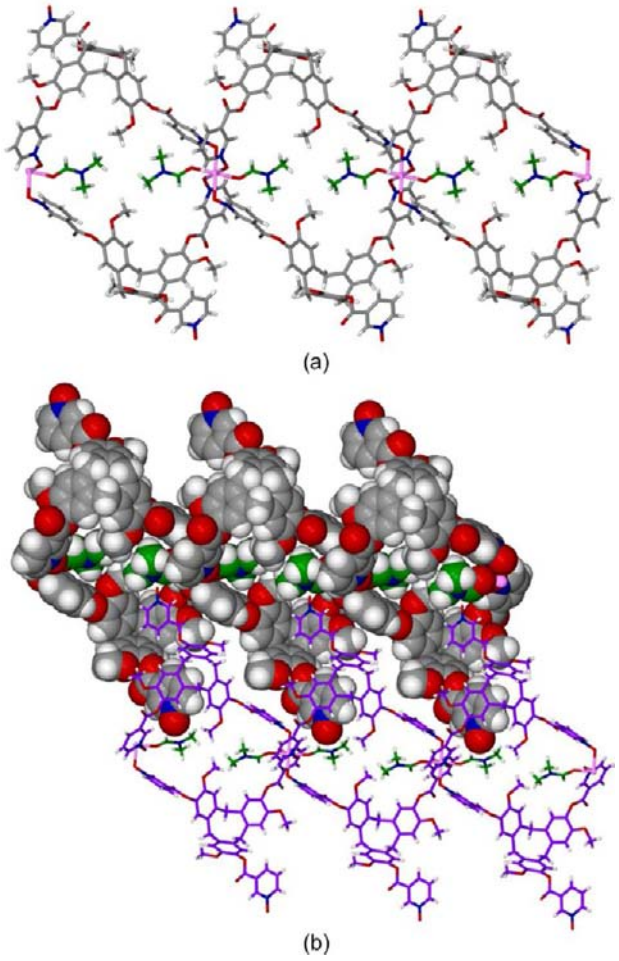

Figure 12. From the crystal structure of $\{[Co(L2)_2(DMF)_2]\cdot 2NO_3\cdot 4(DMF)\cdot H_2O\}_\infty$ **12**. (a) Doubly bridged $[Co(L2)_2(DMF)_2]^{2+}$ coordination chain, DMF ligands shown in green; (b) Interchain hand-shake host–guest interactions.

isotropically. Complex **4** was refined with a block matrix refinement and number of bond length and flat restraints, some solvent was refined at half occupancy, one BF_4^- was refined with disordered F positions and some solvent and the anions were refined isotropically. In complex **5**, one DMF was refined isotropically and disordered over two positions with a shared N atom. For complex **9** the B–F and some C–C and C–N distances of NMP molecules were restrained at chemically reasonable lengths, and the BF_4^- and some NMP molecules were refined isotropically. Complex **12** was analyzed using synchrotron data, and one DMF was refined isotropically.

CONCLUSION

Pyridyl appended cyclotriguaiacylene host molecules can be converted into their pyridyl-*N*-oxide analogues through oxidation with *m*-CPBA. Tris(isonicotinoyl-*N*-oxide)-cyclotriguaiacylene (L1) forms 3,6-connected coordination polymers with a variety of transition metal cations, in particular forming the rare 2-D kagome dual and an example of a pyrite-like 3-D network with Ag(I). Complex $\{[Ag_3(NMP)_6(L1)_2]\cdot 3(ClO_4)\}_\infty$ is decorated with $Ag(NMP)_3$ moieties to form an unusual argentophilic linear trimer. More commonly reported network types are found for complexes with tris(nicotinoyl-*N*-oxide)cyclotriguaiacylene (L2) and with tris(2-*N*-oxide-pyridylmethoxy)cyclotriguaiacylene (L3) with 4-connected 4^4 grid structures predominant for L2 and hexagonal 3-connected 6^3 networks for L3.The networks formed by L1 and L2 are in contrast with the behavior of their respective parent host type ligands tris(isonicotinoyl)cyclotriguaiacylene and tris(2-pyridylmethoxy)cyclotriguaiacylene which have also been reported to form complexes with Ag(I). Tris(isonicotinoyl)-cyclotriguaiacylene forms a doubly bridged chain structure with Ag(I),[8] while tris(pyridylmethoxy)cyclotriguaiacylene forms a 3-connected (10–3a) network.[7b] The differing types of network formation are likely due to the different angle of approach to the metal that the pyridyl-*N*-oxide ligand forms with respect to the linear approach of a pyridyl group.

A distinct trend within these complexes is the formation of the self-complementary inclusion motifs which occur when the cavitand ligand does not bind to three metal cations. The pairwise interaction known as the hand-shake motif where the side arm of one ligand is complexed into the molecular cavity of a second ligand and vice versa was prevalent. For these pyridyl-*N*-oxide ligands the motif was supported through π–π stacking interactions and with the polar *N*-oxide groups directed away from the hydrophobic host cavity. This was particularly the case for L2 where the motif was observed within both the crystalline clathrate L2·2NMP and for coordination polymers. In the case of the latter, this host–guest effectively prevented the L2 ligand binding to a metal ion through all three possible ligand sites. This underlines the importance that host–guest interactions play in the self-assembly of coordination polymers when utilizing host-type ligands, and for ligand L2 the π-stacking supported hand-shake interaction appears favorable over additional metal–ligand interactions.

ASSOCIATED CONTENT

Supporting Information

Additional diagrams of crystal structures, TGA and powder XRD traces for selected complexes, and tables of special positions. This material is available free of charge via the Internet at http://pubs.acs.org.

AUTHOR INFORMATION

Corresponding Author

*E-mail: m.j.hardie@leeds.ac.uk.

Notes

The authors declare no competing financial interest.

ACKNOWLEDGMENTS

We thank the EPSRC, the University of Leeds, and the Brotherton Trust (J.J.H.) for financial support. This work was carried out with the support of the Diamond Light Source.

REFERENCES

(1) reviews: (a) Perry, J. J.; Perman, J. A.; Zaworotko, M. J. *Chem. Soc. Rev.* **2009**, *48*, 3018. (b) Noro, S.; Kitagawa, S.; Akutagawa, T.; Nakamura, T. *Prog. Polym. Sci.* **2009**, *34*, 240. (c) Robin, A. Y.; Fromm, K. M. *Coord. Chem. Rev.* **2006**, *250*, 2127. (d) Ockwig, N. W.; Delgado-Friedrichs, O.; O'Keeffe, M.; Yaghi, O. M. *Acc. Chem. Res.* **2005**, *38*, 176. (e) Janiak, C. *Dalton Trans.* **2003**, 2781. (f) James, S. L. *Chem. Soc. Rev.* **2003**, *32*, 276. (g) Robson, R. *Dalton Trans.* **2000**, 3735.

(2) For example: (a) Ehrhart, J.; Planeix, J.-M.; Kyritsakas-Gruber, N.; Hosseini, M. W. *Dalton Trans.* **2010**, *39*, 2137. (b) Liao, W.; Liu, C.; Wang, X.; Zhu, G.; Zhao, X.; Zhang, H. *CrystEngComm* **2009**, *11*, 2282. (c) Olguin, J.; Castillo, A.; Gomez-Vidales, V.; Hernandez-Ortega, S.; Toscano, R. A.; Munoz, E.; Castillo, I. *Supramol. Chem.* **2009**, *21*, 502. (d) Dalgarno, S. D.; Hardie, M. J.; Raston, C. L. *Cryst. Growth Des.* **2004**, *4*, 227. (e) Dalgarno, S. J.; Raston, C. L. *Chem.*

Commun. **2002**, 2216. (f) Webb, H. R.; Hardie, M. J.; Raston, C. L. *Chem.—Eur. J.* **2001**, *7*, 3616. (g) Kleina, C.; Graf, E.; Hosseini, M. W.; De Cian, A.; Fischer, J. *Chem. Commun.* **2000**, 239.
(3) Mough, S. T.; Holman, K. T. *Chem. Commun.* **2008**, 1407.
(4) For example: (a) Konarev, D. V.; Khasanov, S. S.; Vorontsov, I. I.; Saito, G.; Yu Antipin, M.; Otsuka, A.; Lyubovskaya, R. N. *Chem. Commun.* **2002**, 2548. (b) Hardie, M. J.; Raston, C. L. *Angew. Chem., Int. Ed.* **2000**, *39*, 3835.
(5) Abrahams, B. F.; FitzGerald, N. J.; Robson, R. *Angew. Chem., Int. Ed.* **2010**, *49*, 2896.
(6) Yu, J.-T.; Sun., J.; Huang, Z.-T.; Zheng, Q.-Y. *CrystEngComm* **2012**, *14*, 112.
(7) (a) Little, M. A.; Halcrow, M. A.; Harding, L. P.; Hardie, M. J. *Inorg. Chem.* **2010**, *49*, 9486. (b) Sumby, C. J.; Hardie, M. J. *Cryst. Growth Des.* **2005**, *5*, 1321. (c) Ronson, T. K.; Hardie, M. J. *CrystEngComm* **2008**, *10*, 1731. (d) Carruthers, C.; Fisher, J.; Harding, L. P.; Hardie, M. J. *Dalton Trans.* **2010**, 355. (e) Sumby, C. J.; Fisher, J.; Prior, T. J.; Hardie, M. J. *Chem.—Eur. J.* **2006**, *12*, 2945.
(8) Hardie, M. J.; Sumby, C. J. *Inorg. Chem.* **2004**, *43*, 6872.
(9) Carruthers, C.; Ronson, T. K.; Sumby, C. J.; Westcott, A.; Harding, L. P.; Prior, T. J.; Rizkallah, P.; Hardie, M. J. *Chem.—Eur. J.* **2008**, *14*, 10286.
(10) Little, M. A.; Ronson, T. K.; Hardie, M. J. *Dalton Trans.* **2011**, *40*, 12217.
(11) Ronson, T. K.; Nowell, H.; Westcott, A.; Hardie, M. J. *Chem. Commun.* **2011**, *47*, 176.
(12) For example: (a) Xu, G.; Zhang, X.; Guo, P.; Pan, C.; Zhang, H.; Wang, C. *J. Am. Chem. Soc.* **2010**, *132*, 3656. (b) Wei, M.; He, C.; Sun, Q.; Meng, Q.; Duan, C. *Inorg. Chem.* **2007**, *46*, 5957. (c) Bourne, S. A.; Moitsheki, L. J. *Polyhedron* **2007**, *26*, 2719. (d) Manna, S. C.; Zangrando, E.; Ribas, J.; Chaudjuri, N. R. *Dalton Trans.* **2007**, 1383. (e) Zhang, Y.-Z.; Duan, G.-P.; Sato, O.; Gao, S. *J. Mater. Chem.* **2006**, *16*, 2625. (f) Ang, S. G.; Sun, B. W. *Cryst. Grow. Des.* **2005**, *5*, 383. (g) Hill, R. J.; Long, D.-L.; Turvey, M. S.; Blake, A. J.; Champness, N. R.; Hubberstey, P.; Wilson, C.; Schröder, M. *Chem. Commun.* **2004**, 1792. (h) Long, D.-L.; Hill, R. J.; Blake, A. J.; Champness, N. R.; Hubberstey, P.; Proserpio, D. M.; Wilson, C.; Schröder, M. *Angew. Chem., Int. Ed.* **2004**, *43*, 1851. (i) Long, D.-L.; Blake, A. J.; Champness, N. R.; Wilson, C.; Schröder, M. *Chem.—Eur. J.* **2002**, *8*, 2026.
(13) (a) Dalgarno, S.; Warren, J, E.; Atwood, J. L.; Raston, C. L. *New. J. Chem.* **2008**, *32*, 2100. (b) Dalgarno, S. J.; Hardie, M. J.; Atwood, J. L.; Raston, C. L. *Inorg. Chem.* **2004**, *43*, 6351.
(14) Hardie, M. J.; Mills, R. M.; Sumby, C. J. *Org. Biomol. Chem.* **2004**, *2*, 2958.
(15) Henkelis, J. J.; Ronson, T. K.; Harding, L. P.; Hardie, M. J. *Chem. Commun.* **2011**, *47*, 6560.
(16) (a) Ronson, T. K.; Carruthers, C.; Fisher, F.; Brotin, T.; Harding, L. P.; Rizkallah, P. J.; Hardie, M. J. *Inorg. Chem.* **2010**, *49*, 675. (b) Grealis, J. P.; Muller-Bunz, H.; Casey, M.; McGlinchey, M. J. *Tetrahedron Lett.* **2008**, *49*, 1527. (c) Schmuck, C.; Wienand, W. *Synthesis* **2002**, 655.
(17) (a) Yu, J.-T.; Huang, Z.-T.; Zheng, Q.-Y. *Org. Biomol. Chem.* **2012**, *10*, 1359. (b) Shi, Y.-Y.; Sun, J.; Huang, Z.-T.; Zheng, Q.-Y. *Cryst. Grow. Des.* **2010**, *10*, 314. (c) Hu, Q.-P.; Ma, M.-L.; Zheng, X.-F.; Reiner, J.; Su, L. *Acta Crystallogr., Sect. E* **2004**, *60*, o1178. (d) Collet, A.; Gabard, J.; Jacques, J.; Cesario, M.; Guilhem, J.; Pascard, C. *J. Chem. Soc., Perkin Trans. 1* **1981**, 1630.
(18) (a) Wei, W.; Wang, G.; Zhang, Y.; Jiang, F.; Wu, M.; Hong, M. *Chem.—Eur. J.* **2011**, *17*, 2189. (b) Makha, M.; Raston, C. L.; Sobolev, A. N. *Aust. J. Chem.* **2006**, *59*, 260. (c) Brouwer, E. B.; Udachin, K. A.; Enright, G. D.; Ripmeester, J. A.; Ooms, K. J.; Halchuk, P. A. *Chem. Commun.* **2001**, 565.
(19) (a) Ahmad, R.; Hardie, M. J. *Supramol. Chem.* **2006**, *18*, 29. (b) Caira, M. R.; Jacobs, A.; Nassimbeni, L. R. *Supramol. Chem.* **2004**, *16*, 337. (c) Ibragimov, B. T.; Makhkamov, K. K.; Beketov, K. M. *J. Inclusion Phenom. Macrocyclic Chem.* **1999**, *30*, 583.
(20) (a) Liu, X.; Guo, G.-C.; Fu, M.-L.; Liu, X.-H.; Wang, M.-S.; Huang, J.-S. *Inorg. Chem.* **2006**, *45*, 3679. (b) Zhou, Y.; Chen, W.; Wang, D. *Dalton Trans.* **2008**, 1444. (c) Chen., C. Y.; Zeng, J. Y.; Lee, H. M. *Inorg. Chim. Acta* **2007**, *360*, 21. (d) Zhang, J.-P.; Wang, Y.-B.; Huang, X.-C.; Lin., Y.-Y.; Chen, X.-M. *Chem.—Eur. J.* **2005**, *11*, 552. (e) Mohamed, A. A.; Perez, L. M.; Fackler, J. P. *Inorg. Chim. Acta* **2005**, *358*, 1657. (f) Sun, D.; Cao, R.; Weng, J.; Hong, M.; (g) Liang, Y. *J. Chem. Soc., Dalton Trans.* **2002**, 291. (h) Richardson, S.; Steel, P. J. *Aust. J. Chem.* **2002**, *55*, 783.
(21) Yuan, L.; Qin, C.; Wang, X.; Li, Y.; Wang, E. *Dalton Trans.* **2009**, 4169.
(22) Soma, T.; Iwamoto, T. *Inorg. Chem.* **1996**, *35*, 1849.
(23) (a) Tong, G. S. M.; Kui, S. C. F.; Chao, H.-Y.; Zhu, N.; (b) Che, C.-M. *Chem.—Eur. J.* **2009**, *15*, 10777. (c) Hartshorn, C. M.; Steel, P. J. *Inorg. Chem. Commun.* **2000**, *3*, 476. (d) Jin, J.-C.; Wang, Y.-Y.; Zhang, W.-H.; Lermontov, A. S.; Lermontova, E. K.; Shi, Q.-Z. *Dalton Trans.* **2009**, 10181. (e) Che, C.-M.; Yip, H.-K.; Li, D.; Peng, S.-M.; Lee, G.-H.; Wang, Y.-M.; Liu, S.-T. *Chem. Commun.* **1991**, 1615. (f) Yilmaz, V. T.; Soyer, E.; Buyukgungor, O. *Polyhedron* **2010**, *29*, 920.
(24) O'Keeffe, M.; Peskov, M. A.; Ramsden, S. J.; Yaghi, O. M. *Acc. Chem. Res.* **2008**, *41*, 1782.
(25) Blatov, V. A. *IUCr CompComm Newsletter* **2006**, 4.
(26) Addison, A. W.; Rao, T. N.; Reedijk, J.; Vanrijn, J.; Verschoor, G. C. *J. Chem. Soc., Dalton Trans.* **1984**, 1349.
(27) For example: (a) Sun, H. L.; Wang, X.-L.; Jia, L.; Cao, W.; Wang, K.-Z.; Du, M. *CrystEngComm* **2012**, *14*, 512. (b) Song, X.; Zou, Y.; Liu, X.; Oh, M.; Lah, M. S. *New J. Chem.* **2010**, *34*, 2396. (c) Jiang, M.-X.; Zhan, C.-H.; Feng, Y.-L.; Lan, Y.-Z. *Cryst. Growth Des.* **2010**, *10*, 92. (d) Zhang, Z.-H.; Du, M. *CrystEngComm* **2008**, *10*, 1350. (e) Batten, S. R.; Jenson, P.; Kepert, C. J.; Kuroo, M.; Moubaraki, B.; Murray, K. S.; Price, D. J. *J. Chem. Soc., Dalton Trans.* **1999**, 2987. (f) Batten, S. R.; Hoskins, B. F.; Moubaraki, B.; Murray, K. S.; Robson, R. *J. Chem. Soc., Dalton Trans.* **1999**, 2977.
(28) (a) Du, M.; Zhang, Z.-H.; Tang, L.-F.; Wang, X.-G.; Zhao, X.-J.; (b) Batten, S. R. *Chem.—Eur. J.* **2007**, *13*, 2578. (c) Cordes, D. B.; Hanton, L. R. *Inorg. Chem.* **2007**, *46*, 1634. (d) Batten, S. R.; Hoskins, B. F.; Robson, R. *Angew. Chem., Int. Ed. Engl.* **1995**, *34*, 820. (e) Chae, H. K.; Kim, J.; Friedrichs, O. D.; O'Keeffe, M.; Yaghi, O. M. *Angew. Chem., Int. Ed.* **2003**, *42*, 3907. (f) Lee, E. Y.; Jang, S. Y.; Suh, M. P. *J. Am. Chem. Soc.* **2005**, *127*, 6374.
(29) (a) Zheng, S.-R.; Yang, Q.-Y.; Liu, Y.-R.; Zhang, J.-Y.; Tong, Y.-X.; (b) Zhao, C.-Y.; Su, C.-Y. *Chem. Commun.* **2008**, 356.
(30) Gao, E. Q.; Liu, N.; Cheng, A. L.; Gao, S. *Chem. Commun.* **2007**, 2470.
(31) Zhang, L.; Li, Z.-J.; Lin, Q.-P.; Zhang, J.; Yin, P.-X.; Qin, Y.-Y.; Cheng, J.-K.; Yao, Y.-G. *CrystEngComm* **2009**, *11*, 1934.
(32) (a) Zheng, B.; Zhang, D.; Peng, Y.; Huo, Q.; Liu, Y. *Inorg. Chem. Commun.* **2012**, *16*, 70. (b) Cui, P.; Wu, J.; Zhao, X.; Sun, D.; Zhang, L.; Guo, J.; Sun, D. *Cryst. Growth Des.* **2011**, *11*, 5182.
(33) Jiang, T.; Zhang, X. M. *Cryst. Growth Des.* **2008**, *8*, 3077.
(34) Recent examples of 6^3 networks: (a) Chen, S.-S.; Chen, Z.-H.; Fan, J.; Okamura, T.; Bai, Z.-S.; Lv, M.-F.; Sun, W.-Y. *Cryst. Growth Des.* **2012**, *12*, 2315. (b) Hao, H.-J.; Sun, D.; Li, Y.-H.; Liu, F.-J.; Huang, R.-B.; Zheng, L.-S. *Cryst. Growth Des.* **2011**, *11*, 3564. Sun, D.; (c) Luo, G.-G.; Zhang, N.; Xu, Q.-J.; Jin, Y.-C.; Wei, Z.-H.; Yang, C.-F.; Lin, L.-R.; Huang, R.-B.; Zheng, L.-S. *Inorg. Chem. Commun.* **2010**, *13*, 306. (d) Hou, L.; Zhang, J.-P.; Chen, X.-M. *Cryst. Growth Des.* **2009**, *9*, 2415.
(35) Zn complex was twinned, only unit cell parameters given here: monoclinic, $P2_1$, a = 7.9869(14), b = 24.435(5), c = 14.212(2) Å, α = 90.00, β = 99.980(8), γ = 90.00°, V = 2731.7(8) Å^3.
(36) For example: (a) Alajarin, M.; Orenes, R.-A.; Steed, J. W.; Pastor, A. *Chem. Commun.* **2010**, *46*, 1394. (b) Levilain, G.; Coquerel, G. *CrystEngComm* **2010**, *12*, 1983. (c) Bishop, R. *Acc. Chem. Res.* **2009**, *42*, 67. (d) Gil-Hernandez, B.; Hoeppe, H. A.; Vieth, J. K.; Sanchiz, J.; Janiak, C. *Chem. Commun.* **2010**, *46*, 8270. (e) Jacobs, T.; Hardie, M. J. *Chem.—Eur. J.* **2012**, *18*, 267.
(37) (a) Nizhnik, Y. P.; Szemik-Hojniak, A.; Deperasinska, I.; Jerzykiewicz, L. B.; Korabik, M.; Hojniak, M.; Andreev, V. P. *Inorg. Chem.* **2008**, *47*, 2103. (b) Estes, E. D.; Hodgson, D. J. *Inorg. Chem.*

1976, *15*, 348. (c) Williams, R. J.; Watson, W. H.; Larson, A. C. *Acta Crystallogr., Sect. B* **1975**, *31*, 2362. (d) Morrow, J. C. *J. Cryst. Mol. Struct.* **1974**, *4*, 243.
(38) Stemple, N. R.; Watson, W. H. *Cryst. Struct. Commun.* **1975**, *4*, 25.
(39) Recent examples of 4^4 networks: (a) Huang, H.-X.; Tian, X.-Z.; Song, Y.-M.; Liao, Z.-W.; Sun, G.-M.; Luo, M.-B.; Liu, S.-J.; Xu, W.-Y.; Luo, F. *Aust. J. Chem.* **2012**, *65*, 320. (b) Gong, Y.; Qin, J.; Wu, T.; Li, J.; Yang, L.; Cao, R. *Dalton Trans.* **2012**, *41*, 1961. (c) Jia, J.; Blake, A. J.; Champness, N. R.; Hubberstey, P.; Wilson, C.; Schröder, M. *Inorg. Chem.* **2008**, *47*, 8652. (d) Vagin, S.; Ott, A.; Weiss, H.-C.; Karbach, A.; Volkmer, D.; Rieger, B. *Eur. J. Inorg. Chem.* **2008**, 2601.
(40) Palatinus, L.; Chapuis, G. *J. Appl. Crystallogr.* **2007**, *40*, 786.
(41) Sheldrick, G. M. *Acta Crystallogr., Sect. A* **2008**, *64*, 112.
(42) Barbour, L. J. *J. Supramol. Chem.* **2001**, *1*, 189.
(43) Van der Sluis, P.; Spek, A. L. *Acta Crystallogr., Sect. A* **1990**, *46*, 194.
(44) Spek, A. L. *Acta Crystallogr., Sect. D* **2009**, *65*, 148.